Diana Filipa Duarte Lobo
Licenciada em Bioquímica

Cerebrovascular and Blood-Brain Barrier Impairments in Machado-Joseph Disease

Dissertação para obtenção do Grau de Mestre em Genética Molecular e Biomedicina

Orientadores:
Rui Jorge Gonçalves Pereira Nobre, PhD, CNC UC
Catarina Sofia Oliveira Miranda, PhD, CNC UC

FACULDADE DE CIÊNCIAS E TECNOLOGIA
UNIVERSIDADE NOVA DE LISBOA

Setembro, 2017

Diana Filipa Duarte Lobo
Licenciada em Bioquímica

Cerebrovascular and Blood-Brain Barrier Impairments in Machado-Joseph Disease

Dissertação para obtenção do Grau de Mestre em Genética Molecular e Biomedicina

Orientadores:
Rui Jorge Gonçalves Pereira Nobre, PhD, CNC UC
Catarina Sofia Oliveira Miranda, PhD, CNC UC

Setembro de 2017

O trabalho aqui apresentado foi realizado no grupo de investigação do Prof. Doutor Luís Pereira de Almeida, Grupo de Vectores e Terapia Génica do Centro de Neurociências e Biologia Celular, Universidade de Coimbra, Portugal. Este trabalho foi financiado pelo FEDER através do Programa Operacional Regional Centro 2020, do Programa Operacional de Factores de Competitividade (COMPETE 2020) e por Fundos Nacionais através da FCT (Fundação para a Ciência e a Tecnologia) – projectos BrainHealth2020 (CENTRO-01-0145-FEDER-000008), ViraVector (CENTRO-01-0145- FEDER- 022095), CortaCAGs (POCI-01-0145-FEDER-016719) e POCI-01-0145-FEDER-007440, bem como pelos projectos EXPL/NEU-NMC/0331/2012 (FCT) e pelos SynSpread, ESMI e ModelPolyQ no âmbito do EU Joint Programme - Neurodegenerative Disease Research (JPND), os dois últimos co-financiados pelo programa H2020 da União Europeia, GA No. 643417; ainda pela "National Ataxia Foundation" (USA), pela AFM-Telethon (Proj. nº 21163), pelo American Portuguese Biomedical Research Fund (APBRF) e pelo Richard Chin and Lily Lock Machado Joseph Disease Research Fund.

The work presented here was carried out in the research group of Prof. Dr. Luís Pereira de Almeida, Group of Vectors and Gene Therapy of the Center for Neurosciences and Cell Biology, University of Coimbra, Portugal. This work was funded by the ERDF through the Regional Operational Program Center 2020, Competitiveness Factors Operational Program (COMPETE 2020) and National Funds through FCT (Foundation for Science and Technology) - BrainHealth2020 projects (CENTRO-01- 0145-FEDER-000008), ViraVector (CENTRO-01-0145-FEDER-022095), CortaCAGs (POCI-01-0145- FEDER-016719) and POCI-01-0145-FEDER-007440, as well as the EXPL/NMC/0331/2012 (FCT) and the SynSpread, ESMI and ModelPolyQ under the EU Joint Program - Neurodegenerative Disease Research (JPND), the last two co-funded by the European Union H2020 program, GA No.643417; by National Ataxia Foundation (USA), AFM-Telethon (Proj. nº 21163), the American Portuguese Biomedical Research Fund (APBRF) and the Richard Chin and Lily Lock Machado-Joseph Disease Research Fund.

Acknowledgments

No geral, quero demonstrar a minha mais sincera gratidão a todos os que de uma maneira ou outra contribuíram para que este trabalho fosse possível, tanto a nível profissional como pessoal.

Em primeiro lugar, agradeço ao Professor Doutor Luís Pereira de Almeida por me ter dado a oportunidade de realizar este trabalho no grupo de Vectores e Terapia Génica do Centro de Neurociências da Universidade de Coimbra. Queria também agradecer toda a disponibilidade, simpatia e conhecimento partilhado ao longo deste ano.

Aos meus orientadores, Doutora Catarina Miranda e Doutor Rui Nobre, por me terem aceitado como sua aluna, mas também por toda a atenção, disponibilidade e paciência. Em particular, agradeço todo o conhecimento científico transmitido. A eles devo também parte do trabalho aqui apresentado, nomeadamente tudo o que envolve manipulação de animais.

Gostaria de agradecer também aos Doutores José Sereno, João Castelhano e Miguel Castelo-Branco do Instituto de Ciências Nucleares Aplicadas à Saúde (ICNAS) da Universidade de Coimbra pela disponibilidade em terem realizado as experiências de DCE-MRI apresentadas nesta dissertação. Ao Centro Microscopia de Coimbra (MICC), em particular à Doutora Luísa Cortes e à Doutora Margarida Caldeiras pela disponibilidade e pelos ensinamentos de microscopia. Agradeço também a todos os meus professores que me acompanharam até aqui.

Como não poderia deixar de ser, também gostaria de deixar um agradecimento muito especial a todos os membros do grupo de Vetores e Terapia Génica pelo auxílio mas também pelo bom ambiente de trabalho. Quero deixar um agradecimento especial à Ana Cristina, à Dina, à Inês, à Patrícia e à Sara por me terem ensinado muito e pela amizade que ofereceram à sua "caçula".

À minha família agradeço por tudo, em especial por apesar das muitas dificuldades ter tornado possível este meu percurso académico. Por fim, mas não menos importante, agradeço ao meu "respectivo" pela paciência, pela amizade e motivação, e também deixo um grande obrigado a todos os meus amigos, incluindo uns "Bandalhos" e o Designer Pedro Silva.

Table of Contents

Abstract

Central Nervous System (CNS)-barriers are essential to maintain brain homeostasis, protection and nutrition. Blood-brain barrier (BBB) is mainly constituted by brain endothelial cells, pericytes and astrocytes that restrict the communication between blood and the brain parenchyma. Blood-cerebrospinal fluid barrier (BCSFB) controls molecular exchange between blood and the cerebrospinal fluid in the epithelial cells of choroid plexus. Both barriers express tight junction (TJ) proteins that limit the paracellular permeability between adjacent cells.

In several neurodegenerative diseases, BBB dysfunction has been associated with neuroinflammation and TJs disruption with consequent enhancement of pathogenesis. Machado-Joseph Disease (MJD), also a neurodegenerative disorder, is caused by an expansion in CAG repeats in *MJD1* gene that codifies for mutant ataxin-3 protein and causes neurodegeneration and neuroinflammation.

The aim of this work was to evaluate the cerebrovascular and CNS-barriers integrity in MJD. To accomplish that, we first assessed BBB permeability by quantifying the Evans blue (EB) extravasation in the brain of a transgenic mouse model of MJD. In a second experiment, we aimed at investigating which mechanisms were involved in BBB disruption, by analyzing: the presence of mutant ataxin-3 in cerebellar blood vessels, fibrin extravasation across BBB, and the expression of TJ-associated proteins. Finally, perfusion and vascular permeability were evaluated by Dynamic Contrast Enhanced-Magnetic Resonance Imaging (DCE-MRI).

The results of this work showed that BBB is disrupted in this MJD mouse model, which was demonstrated by Evans blue and fibrin extravasation. Both barriers showed alterations in TJs expression. Occludin was cleaved in both barriers, claudin-5 was upregulated in BBB, whereas ZO-1 showed a tendency to be decreased in BCSFB. Furthermore, it was demonstrated the presence of ataxin-3 aggregates in cerebellar blood vessels. Finally, DCE-MRI confirmed an increased blood volume and higher vascular permeability in MJD mice.

In conclusion, this work demonstrated that cerebrovasculature and CNS-barriers are impaired in MJD.

Keywords: Machado-Joseph Disease (MJD), Neurodegenerative disease, Blood-brain barrier (BBB), Blood-Cerebrospinal Fluid Barrier (BCSFB), Tight Junction (TJ), Dynamic Contrast Enhanced-Magnetic Resonance Imaging (DCE-MRI).

Resumo

As barreiras do sistema nervoso central são essenciais na homeostasia, proteção e nutrição neuronal. A barreira hematoencefálica (BHE) é constituída principalmente por células endoteliais, pericitos e astrócitos, que restringem a comunicação entre o sangue e o parênquima cerebral. A barreira sangue-líquido cefalorraquidiano (BLCR) está localizada nas células epiteliais do plexo coroide e controla a troca de substâncias entre o sangue e o líquido cefalorraquidiano. Ambas as barreiras expressam proteínas *tight junctions* (TJs) que limitam a permeabilidade entre células adjacentes.

Em várias doenças neurodegenerativas, as disfunções na barreira hematoencefálica têm sido associadas a neuroinflamação e alterações das TJs que, consequentemente promovem a progressão da doença. A doença de Machado-Joseph (DMJ) é, também, uma doença neurodegenerativa causada por uma expansão de CAG no gene *MJD1/ATXN3* que codifica a ataxina-3 mutante e leva à neurodegenerescência e neuroinflamação.

O objetivo principal deste trabalho foi avaliar a vasculatura e a integridade das barreiras do sistema nervoso central na DMJ. Para o efeito, num modelo animal da doença, avaliámos a permeabilidade da BHE ao *Evans blue* e, posteriormente, investigámos os mecanismos envolvidos na disrupção da barreira, analisando: a presença de ataxina-3 mutante em vasos sanguíneos do cerebelo, a extravasão da fibrina e a expressão das TJs. Por fim, a permeabilidade vascular foi ainda analisada por ressonância magnética.

Os resultados deste trabalho demonstraram a rutura da BHE neste modelo animal, que foi evidenciada pela extravasão de *Evans blue* e fibrina. Ambas as barreiras mostraram alterações na expressão das TJs. A ocludina foi clivada em ambas as barreiras, a claudina-5 está aumentada na BHE e a ZO-1 mostrou-se tendencialmente reduzida na BLCR. Para além disso, a ataxina-3 mutante foi detectada em vasos sanguíneos do cerebelo. A análise por ressonância magnética mostrou ainda um aumento no volume sanguíneo e confirmou o aumento da permeabilidade vascular no cerebelo de animais transgénicos.

Em conclusão, este trabalho demonstrou que existem alterações na vasculatura e nas barreiras do sistema nervoso central na DMJ.

Palavras-chave: Doença de Machado-Joseph (DMJ), Doenças Neurodegenerativas, Barreira Hematoencefálica (BHE), Barreira Sangue-Líquido Cefalorraquidiano (BLCR), Proteínas *tight junctions* (TJ), Ressonância Magnética.

Abbreviation List

AJ	Adherens Junction
a.u.	Arbitrary Units
AUC	Area Under the Curve
BBB	Blood-brain Barrier
BCSFB	Blood-Cerebrospinal Fluid Barrier
BSA	Bovine Serum Albumin
CAG	Cytosine, Adenine, Guanine
CD31	Cluster of Differentiation 31
CNS	Central Nervous System
CoIV	Collagen IV
CSF	Cerebrospinal Fluid
DAPI	4',6-diamidino-2-phenylindole
DCE-MRI	Dynamic Contrast Enhanced-Magnetic Resonance Imaging
DCN	Deep Cerebellar Nuclei
EB	Evans blue
HA	Hemagglutinin
JAM	Junctional Adhesion Molecule
MJD	Machado-Joseph Disease
MMP	Metalloproteinase
PBS	Phosphate Buffered Saline
PolyQ	Polyglutamine
ROI	Region of Interest
SCA	Spinocerebellar Ataxia
SEM	Standard Error of Mean
Tg	Transgenic
TJ	Tight Junction
VEGF	Vascular Endothelial Growth Factor
WT	Wild Type
ZO	Zonula Occludens

Figures Index

Table index

1. Introduction

1.1 Central Nervous System (CNS)-barriers

The Central Nervous System (CNS) homeostasis is essential for the reliable transmission of chemical and electrical signals among neurons, allowing the regulation of defined neurotransmitters and ionic concentrations around synapses and axons. This homeostasis is mainly accomplished by the barrier systems and extracellular fluids that surround the CNS, which simultaneously protects it from circulating toxins and participates in immune surveillance, reviewed in (Abbott et al 2010).

Thereby, CNS cells have controlled access to peripheral fluids through three major barriers: 1) the Blood-brain barrier (BBB); 2) the blood-cerebrospinal fluid barrier (BCSFB); 3) and the arachnoid epithelium of the meninges. BBB is an interface between blood and the brain parenchyma interstitial fluid, constituted mainly by brain endothelial cells which form brain capillaries. In order to limit contact between blood and the cerebrospinal fluid (CSF), choroid plexus epithelial cells enclose the fenestrated capillaries constituting the BCSFB. Another distinct barrier is formed by the avascular arachnoid epithelium of the meninges, sealing the subarachnoid space filled with CSF from fenestrated capillaries of dura mater. CNS barriers are reviewed in (Saunders et al 2008).

The CSF is predominantly secreted by the choroid plexus of lateral ventricles, circulating through all the four ventricles and through the subarachnoid space, being then absorbed into the venous outflow system (Sakka et al 2011). The contribution of the CSF to CNS homeostasis relies on the communication with brain parenchyma interstitial fluid, which regulates electrolyte balance, circulation of active molecules and promotes elimination of waste products.

Circumventricular organs (area postrema and median eminence, neuro-hypophysis, pineal gland, sub-fornical organ and lamina terminalis) constitute sites of physiological communication with periphery, being responsible for food intake and body temperature regulation. However, they do not represent a blood-CNS barrier (Weiss et al 2009).

1.2 The blood-brain barrier (BBB)

BBB concept was firstly introduced by Lena Stern to describe a complex structure located in the blood vessels of the CNS (Stern & Gautier 1921). Despite the fact that brain endothelial cells are the central element of BBB, they are integrated in a functional concept of the brain designated as “neurovascular unit”, which is essential for BBB development and function. Although being referred as a barrier between systemic circulation and brain parenchyma, it also functions as a selective carrier of blood components required for CNS physiology.

1.2.1 Physiological functions of BBB

BBB constitutes a barrier at several levels: paracellular, transcellular and through efflux transporters. At paracellular level, intercellular junctional complexes restrict molecular and cellular transit between adjacent brain endothelial cells, assuring a physical barrier between blood and the brain interstitial fluid. In addition, brain endothelial cells in BBB limit transcellular movement of molecules in and out of brain tissue through specific transporters and restricted vesicular transport. Besides control of paracellular and transcellular movement, some molecules that are capable to cross BBB are removed back to the blood by efflux transporters expressed in the BBB. These transporters allow ion and neurotransmitter regulation, independently of oscillations in the blood concentration (Abbott et al 2010).

BBB also controls protein content of the brain tissue, which is much lower than plasma, avoiding infiltration of plasma proteins such as albumin, fibrin and pro-thrombin that can damage neural tissue through induction of neuroinflammation. For instance, thrombin and plasmin in the brain can lead to glial activation and albumin induces astrocyte proliferation, both resulting in glial scar formation (Gingrich & Traynelis 2000, Nadal et al 1995).

Moreover, since communication between the periphery and CNS is essential for body homeostasis, namely to provide brain nutrition, BBB acts as a carrier for the exchange of some molecules from blood, through passive diffusion or selective transporters in brain endothelial cells (Abbott et al 2010).

In conclusion, BBB is a complex and dynamic structure adapting its functions in response to the needs of CNS in healthy and disease conditions.

1.2.2 Anatomical features: Neurovascular Unit

The concept of neurovascular unit has been defined to integrate the components that are essential to all functional roles of the CNS, including BBB dynamism (Zlokovic 2011). The neurovascular unit is constituted mainly by vascular cells (endothelial cells, pericytes and vascular smooth muscle cells), glia (astrocytes, microglia, and oligodendrocytes), neurons and the basement membrane. Brain endothelial cells are covered by endothelial basement membrane, which in part is bordered by pericytes. The parenchymal basement membrane encloses the perivascular space along with the astrocytic end-feet. Astrocytes communicate with both neurons and brain endothelial cells, enabling the communication among the different neurovascular unit components (Lecuyer et al 2016) (see Figure 1.1).

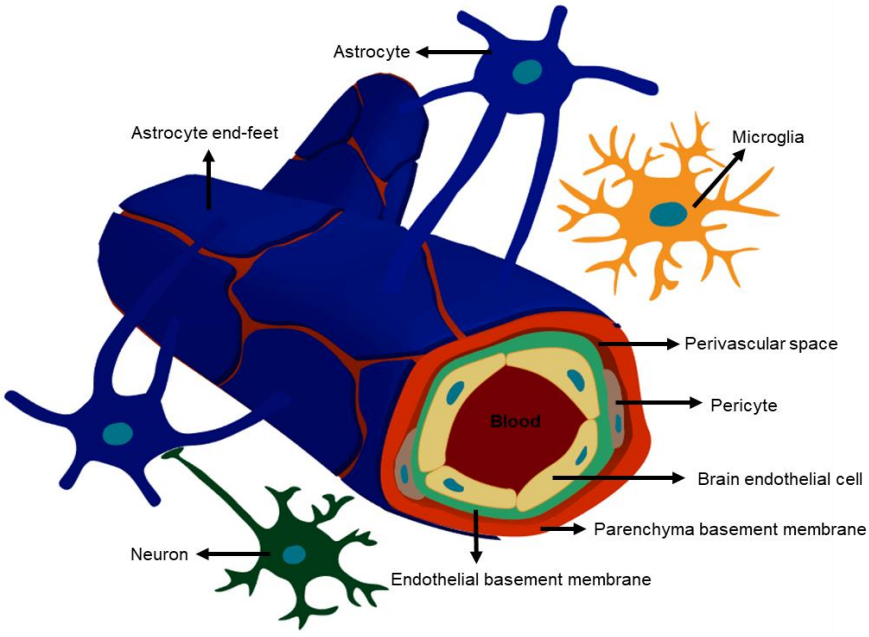

Figure 1.1. Neurovascular unit. Brain endothelial cells of capillaries are enrolled in the endothelial basement membrane and partially covered by pericytes. Surrounded by the parenchyma basement membrane is the perivascular space. Astrocytes contact with brain endothelial cells through their terminals called end-feet. Other intervenients in the neurovascular unit organization are microglia and neurons.

Brain endothelial cells

Brain endothelial cells constitute the larger interface between blood and the brain. These specific cells are distinct from other endothelial cells in what concerns their morphology and function. The principal morphologic difference is the absence of fenestrations due to junctional

complexes, namely tight junctions (TJs) and adherens junctions (AJs), which lead to low paracellular diffusion (Feletou 2011). However, other phenotypic variations differentiate brain endothelium from the remaining endothelial cell types, such as the larger size and the higher amount of cytosolic mitochondria, low levels of pinocytotic vesicles and absence of lysosomal fusion with endocytic vacuoles (Bernacki et al 2008). Another phenotypic feature is the expression of drug and neurotransmitter metabolizing enzymes, such as acetylcholinesterase, alkaline phosphatase, gamma-glutamyl transpeptidase and monoamine oxidases. This enzymatic activity provides protection against high levels of neurotransmitters in the brain, which can damage neuronal tissue, so as other damaging molecules (Wilhelm et al 2011).

Moreover, brain endothelial cells membrane receptors and transporters show distinct expression in luminal (blood) and abluminal (CNS) sides, which enable an unidirectional route of transport across BBB for specific molecules (Banks 2016). The luminal membrane is also distinct from the abluminal one due to a negative charge that is conferred by a glycocalyx coverage, a mesh of proteoglycans, glycosaminoglycans, glycoproteins and glycolipids (van den Berg et al 2006). Glycocalyx maintains BBB integrity by preventing the movement of macromolecules (based on their charge) to the endothelial surface, influencing flow resistance, protecting brain endothelial cells from oxidative stress and preventing the contact between endothelium and red blood cells, platelets and leukocytes. In normal conditions, leukocytes cannot interact with their receptors in brain endothelial cells, thus avoiding their infiltration into the CNS (Kolarova et al 2014). In addition, inflammatory responses are also modulated by glycocalyx, since it can bind to cytokines and, consequently, restrict them to interact with endothelial cell receptors (Reitsma et al 2007). On the other hand, glycocalyx acts as a sensor of biochemical and mechanical forces of blood, transducing it into conformational changes and, consequently, into endothelial cellular responses (Reitsma et al 2007).

Therefore, junctional complexes, glycocalyx and the different distribution of abluminal and luminal receptors give rise to brain endothelial cell polarization, a phenotypic characteristic translated into unique endothelial functions, such as unidirectional transport.

Astrocytes

Astrocytes have multiple functions in the CNS that are essential to many metabolic processes, including: the modulation of synaptic transmission, neurotransmitter uptake and promotion of neurovascular coupling as reviewed in (Cabezas et al 2014, Newman 2003). In CNS, two main types of astrocytes have been described: the protoplasmic astrocytes, which are present in grey matter, around neuronal bodies and synapses, and the fibrous astrocytes present in the white matter associated with Ranvier nodes and oligodendroglial cells (Oberheim et al 2012).

Protoplasmic astrocytes have cytoplasmic appendices, whose endings, called end-feets, interact with both neurons and brain endothelial cells, forming another layer of the neurovascular unit (see Figure 1.1). Although brain endothelium is separated from astrocytes by pericytes and basement membrane, connexins allow for the communication between these two cell types (Winkler et al 2011). The contact with brain endothelial cells during neurodevelopment is responsible for promoting barrier properties, namely polarization of these cells by maintaining TJ and cytoskeleton-associated proteins integrity (Michele & Campbell 2003).

Moreover, as a part of the neurovascular unit, astrocytes synchronize neuronal metabolic demands with local cerebral blood flow. They control exchanges between the nervous system and the vasculature, participate in the formation of parenchymal basement membrane and modulate junctional complexes expression by brain endothelium (Anderson & Nedergaard 2003, Janzer & Raff 1987). Paracrine regulation of BBB by astrocytes is a result of signaling molecules release, such as vascular endothelial growth factor (VEGF), a pro-angiogenic factor that influences brain endothelium growth and glial-derived neurotrophic factor, which specifically induces the expression of the TJ protein claudin-5 in brain endothelial cells (Almutairi et al 2016, Igarashi et al 1999, Shibuya 2008).

Astrocytes also secrete key proteins of the parenchymal basement membrane, as described below (Proctor et al 2005, Sixt et al 2001). Another product released by astrocytes is transforming growth factor-β that has been described to have a dual role in BBB. On one hand, it stabilizes the barrier through the modulation of the expression of P-glycoprotein efflux transporter, which eliminates xenobiotics from CNS (Dohgu et al 2004). On the other hand, transforming growth factor-β is associated with neuroinflammation in diseases such as Alzheimer's and multiple sclerosis (Lecuyer et al 2016). Furthermore, when activated, astrocytes can stimulate the ubiquitin-proteasome system, leading to degradation of TJ proteins (Chang et al 2015, Filous & Silver 2016).

Pericytes

Pericytes are found enwrapped in pre-capillary arterioles, capillaries, and post-capillary venules (Winkler et al 2011). As part of the neurovascular unit, these cells are located between brain endothelial cells and astrocytes, covering part of capillary outer surfaces (Sims 1991) (see Figure 1.1). Contact spots of pericytes with brain endothelium are provided by gap junctions and AJs, where there is no basement membrane (Cuevas et al 1984, Sa-Pereira et al 2012, Winkler et al 2011). During development, pericytes promote angiogenesis by secretion of angiogenic factors. Simultaneously, they respond to platelet-derived growth factor B, which is secreted by brain endothelial cells as a recruitment signal to pericytes (Darland et al 2003, Winkler et al 2011). Besides, pericyte attachment to brain endothelium is promoted by notch signaling, by upregulation of an adhesion protein, N-cadherin (Li et al 2011). Like astrocytes, pericytes maintain barrier properties and influence the expression of TJ-associated proteins (Bonkowski et al 2011, Haseloff et al 2005). However, these effects may occur indirectly, since it has been demonstrated that pericytes act on brain endothelium through the induction of astrocyte polarity and also inhibition of transcellular vesicular trafficking, which is important to control BBB permeability (Armulik et al 2010, Daneman et al 2010).

In addition to their vital role during embryogenesis, pericytes remain crucial in adulthood, namely due to brain endothelium stabilization and maturation, establishment of barrier properties and basement membrane maintenance (Allinson et al 2012, Jeansson et al 2011). In fact, pericytes contribute to basement membrane integrity through the regulation of laminin production and fibronectin secretion (Stratman et al 2009).

Moreover, pericytes are mediators of neurovascular coupling, since they are responsive to vasoactive substances, expressing contractile proteins and vasoactive agents. These substances allow for modulation of capillary blood flow in response to CNS needs (Hamilton et al 2010).

Pericyte phagocytic properties were also suggested to be important in BBB disruption models, due to the participation in the clearance of neurotoxic circulating plasma proteins, including immunoglobulins, fibrin and albumin (Winkler et al 2014, Yates et al 2017).

Basement membrane

BBB integrity is also maintained by both parenchymal and endothelial basement membranes, which provide cell adhesion, structural support and a signaling interface between brain endothelial cells and the surrounding environment (see Figure 1.1). Endothelial basement membrane surrounds pericytes and brain endothelial cells, whereas parenchymal basement membrane delineates perivascular space filled with interstitial fluid.

The main basement membranes constituents are collagen IV (CoIV), fibronectin, laminins, agrin, nidogen-1 and 2 and heparan sulfate proteoglycans (Morris et al 2014). CoIV, produced by brain endothelial cells, pericytes and astrocytes, confer mechanical resistance to basement membrane and stabilize it, retaining laminins (Poschl et al 2004). Laminins are essential to pericytes function, which in turn regulate the expression of these basement membrane glycoproteins (Armulik et al 2010). Another basement membrane glycoprotein, fibronectin, is also secreted by astrocytes, pericytes and brain endothelial cells and its insoluble

form acts as a linker between basement membrane and plasma membrane of both pericytes and brain endothelial cells (Almutairi et al 2016, Cuevas et al 1984, Tilling et al 1998). Additionally, heparin sulfate proteoglycan agrin, is crucial to maintain BBB integrity through stabilization of AJs and TJs proteins (Steiner et al 2014). Integrins and growth factors provide communication between basement membrane components and cells attachment, forming a dynamic basement membrane (Yurchenco 2011). The dynamism is also accomplished by MMPs (metalloproteinases) and its inhibitors that degrade or limit basement membrane degradation, respectively, both in physiological and inflammatory conditions (Weiss et al 2009, Yong 2005).

Neurons

Despite being the basic building block of the CNS, neurons' influence in the BBB activity is still poorly understood. However, it is known that these cells modulate blood vessel function (Cardoso et al 2010). In fact, the contact of neuronal projections with astrocytes and brain endothelial cells induces the regulation of cerebral blood flow by neuronal mediators, which is mainly accomplished by noradrenergic, serotonergic and cholinergic neurons, among others (Hawkins & Davis 2005, Weiss et al 2009). However, a lot of knowledge on this subject is still lacking and needs further investigation.

Microglia

Microglia represents another component in the barrier established between endothelium and neurons. Its high proximity with BBB starts during development in which microglia release VEGF that stimulates angiogenesis, which is reviewed in (Arnold & Betsholtz 2013). In an adult brain, microglia function as part of the immune system, alternating between the inactive form and the activated one. However, in pathological conditions, activated microglia promotes disease progression and BBB breakdown (Dudvarski Stankovic et al 2016). This fact contradicts the idea of an immune-privileged CNS, since microglia is capable of phagocyting microorganisms, whole neurons and even parts of blood vessels (Brown & Neher 2014, Jolivel et al 2015). Accordingly, microglia act as a defense line in the perivascular space, protecting brain from harmful molecules that can cross BBB.

1.2.3 Junctional complexes in the BBB

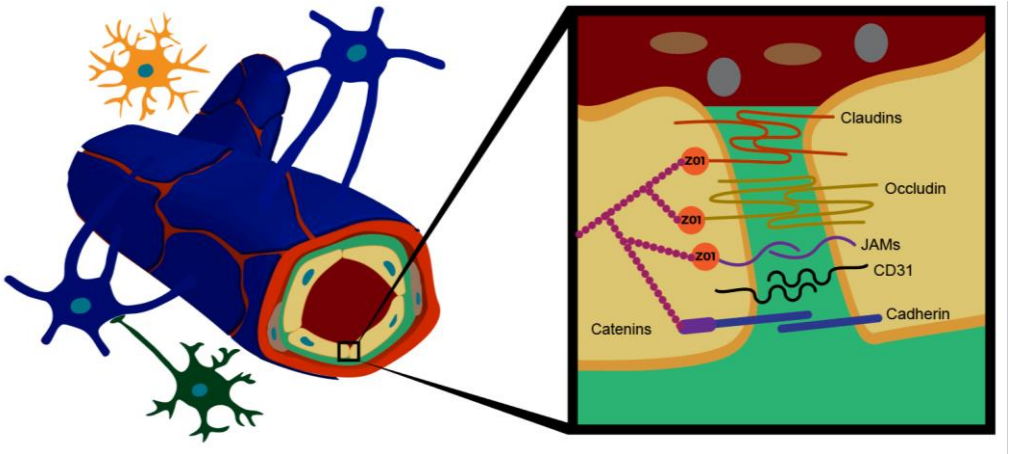

Figure 1.2. Junctional complexes. TJs between adjacent brain endothelial cells are constituted by transmembrane proteins (claudins, occludin and junction adhesion molecules), which are attached to actin cytoskeleton by cytoplasmic accessory proteins, such as zonula occludens-1 (ZO-1). AJs are mainly formed by the transmembrane proteins cadherins and catenins that are bound to the cytoskeleton. JAM= Junctional Adhesion Molecule; CD31= Cluster of Differentiation 31.

The endothelium of brain capillaries has barrier features mainly due to the formation of junctional complexes, including TJs and AJs (Figure 1.2). These intercellular protein complexes lead to low paracellular permeability between adjacent brain endothelial cells and participate in the polarization of these cells. Additionally, gap junctions have also been identified at the BBB, allowing for a tight communication between brain endothelium cells and pericytes through proteins of the connexin family (Nagasawa et al 2006, Rodrigues & Granger 2015). Gap junction plaques provide neighboring brain endothelial cells with ions and small molecules, contributing for the transmission of intercellular signals between adjacent cells (Stamatovic et al 2016). It was shown that in *Drosophila,* gap junctions are essential for the coordinated signaling established in BBB glia (Speder & Brand 2014).

1.2.3.1 Tight junction (TJ)

In the BBB, TJs confer a high electrical resistance of approximately 1800Ωcm2 (Bazzoni & Dejana 2004). Structurally, TJs are constituted by a group of transmembrane adhesion proteins (occludin, claudins and junctional adhesion molecules) and accessory cytoplasmic proteins like zonula occludens (ZO) and cingulin, among others. Accessory cytoplasmic proteins are responsible for linking transmembrane proteins to the actin cytoskeleton, providing TJs with intracellular signaling and physical support (Stamatovic et al 2016) (Figure 1.2).

Multiple cells of the neurovascular unit modulate the formation and maintenance of TJ, namely astrocytes, pericytes and neurons (Abbott et al 2010). Alterations in intracellular and extracellular calcium concentration affect TJs assembly and, consequently, BBB permeability. Extracellular calcium signaling cascade involves phosphokinase-C and heterotrimeric G protein; when extracellular calcium is removed, BBB permeability increases (Stevenson & Begg 1994). In turn, intracellular calcium regulates the proximity of adjacent brain endothelial cells by affecting cytoplasmic TJ proteins location, such as ZO-1. In the absence of intracellular calcium, ZO-1 is not localized in the membrane, where it exerts its function (Stuart et al 1994). In addition, phosphorylation of TJ proteins constitutes to signaling mechanisms of its regulation that finally contribute to BBB dynamism (Huber et al 2001).

Claudins

Claudins are the major component of TJs. They are phosphoproteins with four transmembrane domains and a molecular weight of around 22 kDa. These proteins attach adjacent brain endothelial cells through claudin-claudin hemophilic interactions, while the carboxylic end is connected to cytoplasmic ZO proteins (Bernacki et al 2008) (Figure 1.2). Despite the existence of 26 isoforms of claudins, the most abundant and relevant one in BBB is claudin-5, whose absence leads to disruption of this barrier in mice, despite the presence of other isoforms (Gunzel & Yu 2013). Claudins form size and charge-selective pores and each claudin controls the diffusion of certain molecules' size (Morita et al 1999). For example, claudin-5 allows the diffusion of molecules with <800 Da (Nitta et al 2003). Together, claudins and occludins form heteropolymers and transcellular tracts containing channels for the selective transport of ions and hydrophilic molecules (Matter & Balda 2003). Claudin phosphorylation is one of the regulation forms of TJs' function and consequently regulates BBB permeability. Phosphorylation results in TJs assembly or disassembly, depending on the claudin phosphorylated and the phosphokinase responsible for it. For instance, phosphorylation mediated by phosphokinase-A leads to assembly of claudin-16 but, inversely, leads to claudin-3 disassembly (Findley & Koval 2009). On the other hand, myosin light chain kinase-mediated phosphorylation has been associated with an increase of BBB permeability, in inflammation conditions, due to claudins disassembly (Haorah et al 2005). This reflects the extraordinary complexity of these structures as well as the tight physiological regulation that they require.

Occludin

Occludin is a phosphoprotein with 63 kDa and four transmembrane domains, which regulates paracellular transport (Hirase et al 1997). Together with claudin, the two extracellular loops of occludin constitute the TJ paracellular component, while the cytoplasmic C-terminal domain interacts with cytoplasmic ZO proteins (Zlokovic 2008) (Figure 1.2). Furthermore, occludin is a regulatory protein and its localization in the cell modulates BBB integrity (Huber et al 2001). The function of this TJ-associated protein is also regulated through phosphorylation by several kinases. It can be phosphorylated on serine, threonine and tyrosine residues (Bauer et al 2014). For instance, tyrosine phosphorylation prevents occludin binding to ZO cytoplasmic proteins, leading to an increased paracellular permeability since the transmembrane proteins will no longer be linked to actin cytoskeleton (Kale et al 2003). Small G proteins such as Rho also regulate TJs assembly through occludin phosphorylation, promoting an increase in BBB permeability when occludin is phosphorylated (Hirase et al 2001).

Junctional adhesion molecules (JAMs)

Junctional adhesion molecule (JAM)-A, B and C are immunoglobulins with a single transmembrane domain and an extracellular fragment with two immunoglobulin-like loops (Petty & Lo 2002). In the intercellular cleft, they form homotypic cell-cell contacts between adjacent brain endothelial cells, enhancing its adhesion (Bazzoni et al 2000a). In addition, JAM proteins interact with cytoplasmic TJ proteins, like ZO proteins, in order to anchor to the actin cytoskeleton (Bazzoni et al 2000b). They are also involved in regulation of the immune status within the CNS, since they modulate leukocyte migration through BBB due to its close association with platelet endothelial cellular adhesion molecule 1 (also denominated as cluster of differentiation 31 (CD31)) (Martin-Padura et al 1998). Furthermore, a protein with similar structure to JAM, endothelial cell-selective adhesion molecule is also a transmembrane protein associated with extravasation of neutrophils during inflammation (Stamatovic et al 2016, Wegmann et al 2004).

Cytoplasmic proteins involved in TJ formation

In addition to the previous proteins that belong to the intercellular cleft, there are also cytoplasmic proteins that are essential to TJ formation and brain endothelial cells regulation. Cytoplasmic TJ proteins provide not only structural support to BBB and BCSFB, but also integrate several signaling pathways that regulate activity of brain endothelial cells and epithelial cells from choroid plexus and TJs assembly. Some of these are ZO proteins, cingulin, AG-6, 7H6 and others. ZO-1, 2 and 3 are membrane-associated guanyl kinase-like proteins, which connect claudins, occludin and JAM proteins to the actin cytoskeleton, allowing effectiveness of TJs' regulation (Vorbrodt & Dobrogowska 2004). In fact, ZO proteins may even translocate to the nucleus regulating proliferation by interacting with transcription factors (Bauer et al 2014, Betanzos et al 2004). The absence of ZO-1 has demonstrated its relevance at the establishment of junctional proteins placement and angiogenesis, since its knock out leads to lethal phenotype during embryogenesis in mice (Katsuno et al 2008).

ZO-1 has two isoforms: ZO-1 α- and ZO-1 α+. Isoform α- is restricted to endothelium, thus present in BBB, and some atypical epithelial cells, such as renal glomerular podocytes and between Sertoli cells; while isoform α+ is found in most epithelial-cell junctions (Willott et al 1992). With similar functions, the myosin-like phosphoprotein named cingulin, stands between transmembrane proteins and the cytoskeleton, binding to ZO proteins and myosin (Cordenonsi et al 1999). The 7H6 phosphoprotein is associated with the impermeability of the BBB to ions and large molecules (Satoh et al 1996). In conditions of low ATP levels, 7H6 protein dissociates from the other TJ proteins, which leads to an increase of paracellular permeability, demonstrating the dynamic properties of junctional complexes in response to environmental circumstances (Huber et al 2001).

Other cytoplasmic proteins described in the BBB are Ca^{2+}-dependent serine protein kinase, partitioning defective proteins, multi-PDZ-protein 1, membrane-associated guanylate

kinase with inverted orientation of protein-protein interaction domains, small guanosine triphosohateases, G-protein signaling 5, and ZO-1-associated nucleic acid-binding protein. Together, these proteins are responsible for ensuring the integrity of TJs and structural support of the brain endothelium and its regulation (Bernacki et al 2008).

1.2.3.2 Adherens junction (AJ)

In order to allow TJs assembly, it is not only necessary the presence of other junctional complexes, AJs, but also the crosstalk between these two complexes to maintain a dynamic BBB (Tietz & Engelhardt 2015). Consequently, AJs are essential to BBB integrity and its absence leads to barrier disruption (Wolburg & Lippoldt 2002). These junctional complexes are located at the basal region of lateral plasma membrane and mediate paracellular permeability between brain endothelial cells through the stabilization of cell-cell interactions. AJ main proteins are the transmembrane glycoproteins, cadherins, which interact homotipically to enhance adhesion between brain endothelial cells (Takeichi 1995). To anchor cadherins to the actin cytoskeleton, cytoplasmic proteins β and Ɣ-catenins mediate cadherin connection with α-catenin, which in turn interact to actin (Nieset et al 1997). Catenin and vascular endothelial-cadherin have been identified in the human cortex (Vorbrodt & Dobrogowska 2004). CD31 is also present in human AJs, interacting with β-catenin (Matsumura et al 1997).

Regarding the cross-talk between the two types of junctional complexes, interactions of AJs with TJs start during development when AJs initiate cell-cell contacts and promote TJ maturation, maintenance and plasticity (Tietz & Engelhardt 2015). Vascular endothelial-cadherin promotes upregulation of claudin-5 expression. This has been demonstrated due to increased paracellular permeability as a consequence of claudin-5 downregulation, in the absence of vascular endothelial-cadherin (Taddei et al 2008). However, TJ proteins also have a modulation role in AJs, namely ZO-1 essential role in vascular endothelial-cadherin integrity (Tornavaca et al 2015). Furthermore, AJs are also regulated by phosphorylation, namely by tyrosine phosphorylation of β-catenin which results in disruption of this junctional complex (Roura et al 1999).

1.2.4 Routes of transport across BBB

Intact and functional BBB restricts the entry of compounds according with certain factors: high polar surface area, tendency to form more than 6 hydrogen bonds, presence of rotatable bonds in the molecule, a molecular weight higher than 450 Da and a high affinity of binding to plasma proteins. Besides that, molecules with cationic nature have advantage over acids when penetrating BBB, due to the negatively charged glycocalyx of brain endothelium, as reviewed in (Abbott et al 2010).

Nevertheless, one of the main roles of BBB is the regulation of the transport of nutrients, cells and other molecules into and out of the brain. Through paracellular pathway, by crossing TJs, some water-soluble agents can penetrate BBB into the CNS. On the other hand, lipid-soluble molecules can enter the brain passively through transcellular route (Liu et al 2004). Blood gases, oxygen and carbon dioxide diffuse through lipid membranes of brain endothelial cells, depending on their concentration gradient (Abbott et al 2010). Furthermore, there are specific transport systems on the luminal and abluminal membranes, such as solute carriers and ATP-binding cassette transporters. Solute carriers control the transcellular traffic of small hydrophilic molecules, such as glucose, amino acids, nucleosides and choline. ATP-binding cassette transporters transport, with consume of ATP, lipid-soluble substances out of the brain. The most significant of these transporters are Multidrug Resistance-Associated Proteins and Breast Cancer Resistance Proteins (Begley 2004). P-glycoprotein is a Multidrug Resistance-Associated Protein, and it was the first identified in humans in several organs such as the intestine, kidney, pancreas, peripheral immune cells and in BBB (Loscher & Potschka 2005). Its wide activity in the BBB is

demonstrated by its expression in many cells, specifically brain endothelial cells, astrocytes, microglia and pericytes (Beaulieu et al 1997, Lee & Bendayan 2004).

Additionally, specific receptor-mediated transcytosis allows the entry of large molecules, such as insulin and transferrin, using the vesicular trafficking machinery of brain endothelial cells promoted by receptor-ligand interactions (Abbott et al 2006). Conversely, absorptive-mediated transcytosis allow the entrance of molecules into the brain with less specificity than receptor-mediated transcytosis, based only on charge interactions (Jones & Shusta 2007).

Regarding cell movement across BBB, it is known that perivascular space functions as a niche for immune cells, namely mononuclear cells that in the absence of pathology can enter the brain through diapedesis, without rearranging TJ (Bechmann et al 2001). In pathological scenarios, leukocytes, monocytes and macrophages can penetrate BBB by promoting TJs rearrangements, keeping up with microglia (Davoust et al 2008).

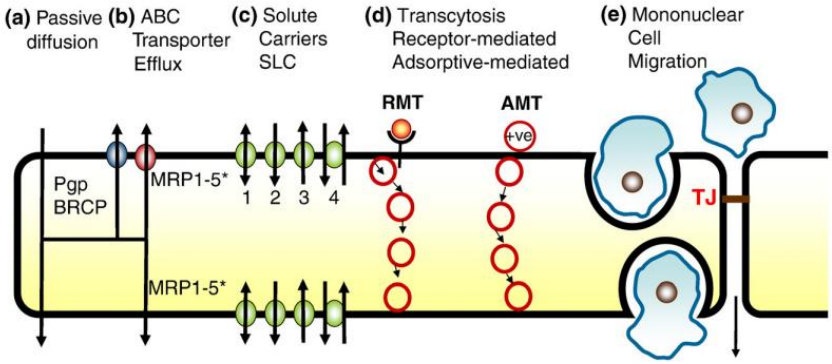

Figure 1.3. Different routes of transport across the BBB. a) Passive diffusion of lipid soluble molecules; b) ATP-binding cassette (ABC) transporter efflux xenobiotics and lipid soluble metabolites; c) Solute carriers (SLC) mediate transport of polar substances; d) Receptor (RMT) and adsorptive- mediated transcytosis (AMT) involves vesicular transport; e) Cell movement may occur through transcellular or paracellular route involving TJ disarrangement. Pgp= P-glycoprotein; BCRP= Breast Cancer Resistance Protein; MRP= Multidrug Resistance Protein. Reviewed in (Abbott et al 2010).

1.3 The Blood-Cerebrospinal Fluid Barrier (BCSFB)

BCSFB is localized in the choroid plexus of cerebral ventricles, being an interface between blood and CSF. Main functions of BCSFB are: to prevent the entry of toxic substances to the CSF, such as toxins; to provide glucose, oxygen, ions and vitamins necessary to CSF production; to absorb and eliminate the waste products from this fluid; to maintain Ca^{2+} homeostasis and hormones transport, as reviewed in (Engelhardt & Sorokin 2009).

Although BBB and BCSFB have a similar function, their structure are quite different. BCSFB is constituted by epithelial cells of the choroid plexus, which are wrapped in the subepithelial basement membrane (see Figure 1.4). The intermediate interstitium separates the basement membrane and the voluminous vasculature, which is formed by fenestrated capillaries. The high content of blood vessels in the choroid plexus produce the high blood flow necessary to CSF production. In addition, these capillaries are highly permeable, in contrast with brain endothelial cells from BBB (Tietz & Engelhardt 2015).

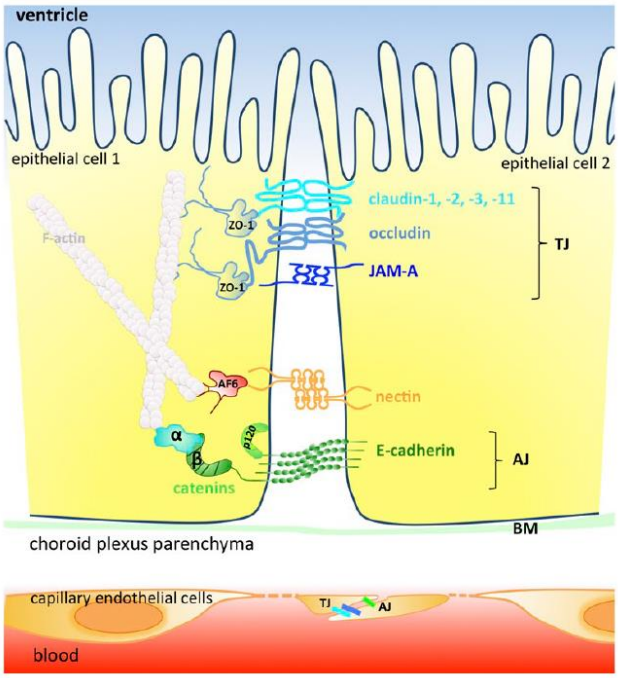

Figure 1.4. Structure of BCSFB and junctional complexes from epithelial cells of the choroid plexus. Distance between adjacent epithelial cells is reduced by the existence of tight junctions (TJ) and adherens junctions (AJ). Claudin- 1, 2, 3 and 11 among others together with occludin and junctional adhesion molecule-A (JAM-A) form the transmembrane component of TJs, whereas zonula occludens-1 (ZO-1) constitutes the cytoplasmic link to the cytoskeleton. AJs are formed by cadherin and catenins. Adapted from (Tietz & Engelhardt 2015).

TJs in BCSFB are expressed in epithelial cells, restricting the paracellular permeability between adjacent cells. However, these junctional complexes in BCSFB are leakier than the ones formed in BBB. In fact, TJ-associated proteins involved in BCSFB are different from BBB. Although there are some common components, such as occludin, they express different claudins and different ZO-1 isoforms. In BCSFB, claudins 1, 2, 3, 9, 11, 19 and 22 are predominantly expressed, so as ZO-1 isoform α+ which is associated with epithelial cells (Liddelow et al 2013); whereas claudins 3, 5 and 12 and ZO-1 isoform α- are associated with the endothelium of BBB (Hawkins & Davis 2005, Willott et al 1992). The epithelial cells of choroid plexus also form AJs between them and express efflux transporters, such as P-glycoprotein (Mealey et al 2008). Besides paracellular flux of molecules, another route of transport of BCSFB is through transcytosis, specially macromolecules, such as transferrin (Xiao & Gan 2013).

1.4 BBB dysfunction in neurodegenerative disorders:

BBB dysfunction is a natural event during aging and occurs mainly due to chronically elevated levels of pro-inflammatory cytokines, such as tumour necrosis factor-α, interleukin-6 and interleukin-1β, which regulate the expression of TJ-associated proteins. In particular, high levels of tumour necrosis factor-α in ageing are associated with TJs loss (Elahy et al 2015). Nevertheless, in some neurodegenerative diseases, the BBB is even more dysfunctional than in normal ageing process. In fact, many of these disorders have a late onset, which in part may be correlated with BBB alterations. Implications and causes of BBB dysfunction in Multiple Sclerosis, Parkinson's, Alzheimer's and Huntington's diseases are discussed below.

Table 1.1. BBB alterations in neurodegenerative diseases. Multiple sclerosis, Parkinson's, Alzheimer's and Huntington's diseases and the respective abnormalities in neurovascular unit, TJs, BBB transporters and in extravasation of some substances from this barrier.

Neurodegenerative Disease	*BBB alteration*	*Reference*
Multiple sclerosis	Astrocyte activation	(Lopes Pinheiro et al 2016)
	Infiltration of activated leukocytes	(Lassmann et al 2007) (Larochelle et al 2011)
	Occludin dephosphorilation and TJ disruption	(Morgan et al 2007)
	Decreased P-glycoprotein levels	(Kooij et al 2010)
	Fibrin extravasation	(Yates et al 2017)
Parkinson's disease	Decreased ZO-1 and occludin expression	(Chen et al 2008)
	Reduced contact between neurons and brain endothelial cells	(Farkas et al 2000)
	Decreased levels of P-glycoprotein	(Kortekaas et al 2005)
Alzheimer's disease	Downregulation of ZO-1 expression	(Kook et al 2013)
	Reduction in pericytes	(Halliday et al 2016)
	Altered amyloid-β clearance	(Deane et al 2004)
	Reduced P-glycoprotein activity	(Deo et al 2014)
Huntington's disease	Increased brain blood vessels density	(Drouin-Ouellet et al 2015)
	Impaired vascular reactivity	(Hsiao et al 2015)
	Decreased levels of occludin and claudin-5	(Drouin-Ouellet et al 2015)
	Redistribution of claudin-5	(Lim et al 2017)

1.4.1 Multiple sclerosis

In multiple sclerosis, neurodegeneration is preceded by demyelination and axonal loss, mainly due to inflammatory and immune system reactions. This may lead to a variety of symptoms, such as muscle weakness, affected vision and coordination, balance impairment and memory loss.

As regulators of BBB function and mediators of inflammation, activated astrocytes have a dual effect in BBB in multiple sclerosis, where their protective role is represented by the production of retinoic acid, which has an antioxidant effect in brain endothelial cells (Mizee et al 2014). Conversely, Pinheiro et al. described BBB dysfunction as an initial event in this disease that further results in astrocyte activation due to the infiltration of toxic molecules in the CNS (Lopes Pinheiro et al 2016). Activated astrocytes are known to release pro-inflammatory cytokines that affect BBB integrity (Lee et al 2012, Lopes Pinheiro et al 2016). In addition, activated astrocytes release monocyte chemoattractant protein-1, a chemokine found to induce TJ degradation (Stamatovic et al 2009). In fact, alterations in junctional complexes were found in the experimental autoimmune encephalomyelitis model for multiple sclerosis. Occludin dephosphorylation, associated with TJ disruption, was demonstrated to be associated with inflammation and to occur prior to BBB disruption, suggesting that it might be a target for signaling processes in this disease model (Morgan et al 2007, Sakakibara et al 1997). Moreover, microvascular P-glycoprotein levels are decreased in multiple sclerosis, possibly affecting the efflux of toxic molecules, such as fibrin that is a neurotoxic blood-born protein affecting multiple sclerosis progression (Kooij et al 2010, Yates et al 2017).

All previously described events lead to BBB disruption documented in this disease. Consequently, it was also demonstrated that activated leukocytes, plasma proteins and inflammatory agents from periphery are able to infiltrate the brain parenchyma through brain capillaries (Bruck et al 1997, Larochelle et al 2011, Lassmann et al 2007). Migration of leukocytes leads to demyelination and boosts BBB permeability, increasing subsequent leukocyte infiltration (Biernacki et al 2004, Seguin et al 2003). Some authors suggested that BBB remains persistently dysfunctional in multiple sclerosis, while others found evidences that BBB dysfunction is transient and dynamic, as a focal reaction in the site of a newly developing inflammatory lesion (Claudio et al 1995, Eisele et al 2016, LeVine 2016).

Furthermore, BCSFB have also been implicated in this disease, since TJ-associated proteins such occludin, ZO-1 and claudins were found downregulated in this disease (Kooij et al 2014).

1.4.2 Parkinson's disease

Parkinson's disease is characterized by motor symptoms and neuropsychiatric disturbances caused by neurodegeneration especially in dopaminergic neurons of substantia nigra. Other pathological hallmark is neuroinflammatory course and immune response that lead to progressive neurodegeneration (Yan et al 2014). At the molecular level, intranuclear aggregates of α-synuclein (Lewy bodies) are formed within neurons and other CNS cells affecting their function. An example of this picture is the accumulation of α-synuclein in astrocytes that disturbs its activity (Song et al 2009).

In Parkinson's patients, dopaminergic neurons of substantia nigra extend their axons to the striatum, the site where *post-mortem* studies have found BBB dysfunction in these patients (Gray & Woulfe 2015). Besides, in the striatum of the 1-methyl-4-phenyl-1,2,3,6-tetrahydropyridine mouse model of Parkinson's disease there was a decreased expression of TJ proteins ZO-1 and occludin associated with enhanced paracellular permeability in brain endothelial cells (Chen et al 2008). This may be explained by microglia activation and pro-inflammatory cytokine expression caused α-synuclein aggregation (Gu et al 2010). Consequently, inflammatory molecules lead to BBB disruption due to the attraction of lymphocytes to the damaged site (Blum-Degen et al 1995, Gonzalez-Scarano & Baltuch 1999). Moreover, in Parkinson's disease there is reduced contact between neurons and brain endothelial cells, which disturb neurovascular coupling essential to BBB function (Farkas et al 2000, Thiollier et al 2016). In the brain endothelial cells, there is evidence that P-glycoprotein, a BBB protein responsible for the removal of toxic compounds out of the brain, has its activity reduced in the midbrain, which can be associated with α-synuclein accumulation (Bartels 2011, Kortekaas et al 2005).

Consequently, BBB disruption can enhance Parkinson's disease progression by inducing apoptotic death of nigral dopaminergic neurons (Rite et al 2007). Loss of integrity of these neurons can be explained by thrombin leakage through BBB into the brain, enhancing an intense inflammatory reaction (Carreno-Muller et al 2003). Another consequence of BBB increased permeability is the impairment in α-synuclein transport across BBB. This transport occurs bidirectionally and is assured by the lipoprotein receptor-related protein-1, which in conditions of systemic inflammation, can lead to the increased uptake of α-synuclein (Sui et al 2014).

Regarding the sequence of events, it is suggested that BBB disruption is an early event, which enhances α-synuclein aggregation due to the leakage of neurotoxic agents (Gray & Woulfe 2015).

1.4.3 Alzheimer's disease

Cognitive decline and loss of memory in Alzheimer's disease result from several events: amyloid-β aggregates forming plaques, tau protein in neurofibrillary tangles, inflammation, neurovascular dysfunction and neuronal loss (Zlokovic 2011). Amyloid-β activates microglia and

astrocytes through Toll-like receptors, leading to the production of reactive oxygen species and cytokines, thus triggering an intense inflammatory response in CNS (Caldeira et al 2017, Guerriero et al 2016). This leads to another Alzheimer's disease hallmark, BBB breakdown with TJ disruption, which has been demonstrated in Alzheimer's disease patients and mouse models of the disease (Kook et al 2013, van de Haar et al 2016).

BBB dysfunction in Alzheimer's disease is, in part, explained by dysregulation of vasoconstrictors and vasodilators, along with oxidative stress in brain endothelial cells, impair BBB structure and function (Aliev et al 2009, Palmer et al 2012, Sole et al 2015). Pericyte reduction leads to short coverage of brain endothelial cells, enhancing vascular dysfunction. Ultimately, neurovascular unit impairment results in BBB disruption and consequent extravasation of immunoglobulin G and fibrin, plasma proteins that are toxic to neurons (Halliday et al 2016). Additionally, Alzheimer's disease has been linked to changes in the expression of TJ proteins. For example, there is disruption of ZO-1 expression, caused by high intracellular Ca^{+} and metalloproteinases levels induced by amyloid-β42 (Kook et al 2013).

On the other hand, an intact BBB may regulate amyloid-β accumulation in the CNS, through receptor-mediated transport mechanisms which control both the efflux and influx of this protein into the brain (Mackic et al 2002). Amyloid-β is exported from the brain across BBB through low-density lipoprotein receptor-related protein 1 and 2 transporter and P-glycoprotein, whereas receptor for advanced glycation end products is responsible for the import to the brain (Bell et al 2007, Lam et al 2001, Storck et al 2016). In Alzheimer's patients, inflammation and oxidative stress disturb amyloid-β transport across BBB (Jaeger et al 2009). Low density lipoprotein receptor-related protein 1 transporter is impaired, resulting in a decreased efflux of amyloid-β out of the brain (Deane et al 2004). In addition, P-glycoprotein is decreased in this disease leading to an impaired amyloid-β clearance (Deo et al 2014). Simultaneously, higher levels of receptor for advanced glycation end products activity promote increased amyloid-β transcytosis into the brain, causing its accumulation in brain parenchyma. Besides, the interaction of these receptors with amyloid-β triggers the intracellular Ca^{2+} signaling cascade and MMPs secretion resulting in TJ disruption (Kook et al 2013, Stuart et al 1996). Consequently, amyloid-β accumulation leads to further paracellular permeability, as explained above. Therefore, in Alzheimer's, an accumulation of other circulating proteins, like immunoglobulins, albumin, fibrinogen and thrombin, was also demonstrated (Halliday et al 2016).

1.4.4 PolyQ diseases: the particular case of Huntington's disease

Polyglutamine (polyQ) diseases are neurodegenerative disorders characterized by the expansion of the cytosine-adenine-guanine (CAG) repeat in genes encoding a long polyglutamine tract in the respective protein, which causes alterations in its function. Huntington's disease, dentatorubral-pallidoluysian atrophy, spinal and bulbar muscular atrophy and spinocerebellar ataxia types (SCA) 1, 2, 3 6, 7 and 17 are the nine members of polyQ diseases (Gatchel & Zoghbi 2005, Matos et al 2011, Shao & Diamond 2007).

Huntington's disease is an autosomal dominant disorder with a CAG repeat expansion in the exon 1 of the huntingtin gene, which leads to a mutant huntingtin protein. This mutated protein forms oligomers, and, ultimately, insoluble aggregates (Scherzinger et al 1997). In both YAC128 and R6/2 transgenic mouse models and human patients, there have been evidences of increased density and decreased size of blood vessels, a fact that is independent from the neuronal loss in Huntington's disease (Drouin-Ouellet et al 2015, Franciosi et al 2012). On the other hand, in both Huntington's animal models and human patients, BBB has shown structural and functional changes resulting in increased permeability (Drouin-Ouellet et al 2015, Franciosi et al 2012).

Aggregates of mutant huntingtin have been found in many cells of the neurovascular unit, including brain endothelial cells and astrocytes (Bradford et al 2009, Waldvogel et al 2015). In the presence of inflammation, astrocytes express this mutant protein and VEGF-A, which causes neurovascular changes that include proliferation of primary brain endothelium, leading to

increased vessel density. Impaired astrocytes may also be responsible for low pericyte coverage as observed by Hsaio et al. (Hsiao et al 2015). Furthermore, it has been demonstrated that mutant huntingtin can be transmitted by a non-cell autonomous mechanism, and that this protein is expressed peripherally by circulating monocytes and leukocytes. Thus, peripheral cells can transport it from blood to the CNS and increase its toxicity in neurovascular unit cells (Drouin-Ouellet et al 2015, Weiss et al 2012). In addition, Huntington's paracellular permeability at BBB is increased due to reduction in TJ-associated protein expression, namely occludin and claudin-5 (Drouin-Ouellet et al 2015). More recently, a study performed in an *in vitro* model of Huntington's disease demonstrated similar levels of claudin-5 expression comparing to control, but showed a redistribution of this protein in the brain endothelial cell. In this case, instead of a typical transmembrane location, claudin-5 was detected in the cytoplasm (Lim et al 2017).

Regarding the sequence of events, it has been suggested that BBB dysfunction in Huntington's disease is a primary event of neurodegeneration, possibly due to the susceptibility of brain endothelial cells to oxidative stress caused by high levels of mutant huntingtin, which may influence cellular energy metabolism (Browne et al 1999, Drouin-Ouellet et al 2015). All of these vascular alterations and BBB damage enhance neurodegeneration and, consequently, Huntington's disease progression, as well as alter brain perfusion and reduce toxin clearance of CNS (Waldvogel et al 2015).

1.5 Machado-Joseph disease (MJD):

1.5.1 Genetics and protein physiology

Also called spinocerebellar ataxia type 3 (SCA3), Machado-Joseph disease (MJD) is the most common autosomal dominant spinocerebellar ataxia worldwide. In this polyQ disorder, the mutated protein is ataxin-3, encoded in *MJD1* gene on chromosome 14q32.1 (Takiyama et al 1993). The exon 10 of this gene contains CAG repeats encoding for a polyglutamine fragment at the C-terminus, interrupted by a single lysine. While in healthy individuals, the *MJD1* gene contains 10 to 51 CAG repeats, in MJD patients the number of CAG repeats reaches 55 to 87 repeats (Kawaguchi et al 1994, Lima et al 2005). When the number of CAG triplets is between these two intervals, the disease shows incomplete penetrance (Ichikawa et al 2001). Although it is not completely understood, polyQ expansion within mutated ataxin-3 possibly leads to its toxic gain of function (Nóbrega 2012, Schmidt et al 1998). MJD usually has a late onset, with the first symptoms arising between the age of 20 and 50 years. Some authors suggest that age onset is negatively correlated with the number of CAG repeats (Jardim et al 2001). Due to the instability of mutant alleles, the number of repeats may increase between generations leading to an anticipated disease onset and the possibility of mosaicism related to the number of glutamines (Igarashi et al 1996, Maciel et al 1997, Sequeiros & Coutinho 1993). The extremely rare cases of homozygosity of this mutation show considerable more severity, suggesting a gene dosage effect (Carvalho et al 2008).

Ataxin-3 expression has been described in many different cell types, throughout peripheral and CNS tissues, being present in the cytoplasm, nucleus and mitochondria (Paulson et al 1997, Trottier et al 1998). Structurally, ataxin-3 contains a catalytic Josephin domain located in the N-terminus of the protein with ubiquitin interacting motifs, whereas a flexible C-terminus contains the polyQ fragment (Mao et al 2005, Masino et al 2003). This protein can undergo post-transcriptional modifications, being mono- or oligo-ubiquitinated, enhancing its deubiquitinating activity (Todi et al 2009). Ataxin-3 can also experience proteolysis by caspases and calpains, for example, during cell apoptosis, in which a polyQ fragment is released (Berke et al 2004).

The wild-type form (non-expanded) of ataxin-3 has at least 20 different isoforms, the lengthiest form having 42 kDa. Though its functions are still poorly understood, it is known that ataxin-3 is a deubiquitinating enzyme involved in protein quality control, especially within the proteasome system, regulating the ubiquitinated status of many proteins; furthermore, it is also

involved in transcription regulation, cytoskeleton organization and myogenesis (Bettencourt et al 2010, do Carmo Costa et al 2010, Matos et al 2011, Todi et al 2009). In fact, inhibition of ataxin-3 catalytic activity leads to an increase in polyubiquitinated proteins, comparable to the levels observed when proteasome is inhibited (Berke et al 2005). Recently, ataxin-3 was also associated with autophagy, the process of programmed degradation of cellular components. Interaction of ataxin-3 with beclin-1, a crucial element of autophagy, prevent beclin-1 degradation by proteasome and enables its activity in autophagy (Ashkenazi et al 2017). Moreover, in *Caenorhabditis elegans*, absence of ataxin-3 ortholog showed dysregulated transcription in 1,4 % of the genome, mainly in genes related to cell structure, mobility components, signal transduction, among others (Rodrigues et al 2007). *In vitro* studies suggest that ataxin-3 interacts with histones and works as a corepressor in transcription regulation (Li et al 2002). Its involvement in cytoskeleton organization is suggested by its association with constituents of the microtubule organizing center, such as dynein, histone deacetylase 6, tubulin, etc, and is supported by studies with cell lines in which absence of ataxin-3 results in cytoskeleton disorganization (Burnett & Pittman 2005, Mazzucchelli et al 2009, Rodrigues et al 2007).

1.5.2 Clinical features

MJD is a heterogeneous disease affecting various systems. The most common are cerebellar, pyramidal, extrapyramidal, motor neuron and oculomotor systems. The first symptoms start with unsteadiness upon turning, gait imbalance and progress gait ataxia, limb incoordination and dysarthria with scanning speech. Some of the relevant clinical features to diagnosis are progressive cerebellar ataxia, pyramidal signs associated with extrapyramidal signs or peripheral amyotrophy, with gait and limb ataxia being the most disable features (Paulson 2007). Less frequent are external progressive ophthalmoplegia, dystonia, intention fasciculation-like movements of facial and lingual muscles and bulging eyes. Due to the heterogeneity of the disease, MJD can be divided in three main types. Type 1 refers to the earlier onset, with a mean of 24.3 years, and fastest progression including pyramidal and extrapyramidal signs, such as dystonia and bradykinesia, associated with cerebellar ataxia and ophthalmoplegia. Type 2 has an intermediate onset (mean of 36 years), also including cerebellar ataxia and ophthalmoplegia and may present pyramidal signs. Patients with type 3 MJD have a later onset (mean of 50 years) and differ from type 2 due to the peripheral alterations; besides, it may include slight pyramidal and extrapyramidal signs (Bettencourt & Lima 2011). Less frequent, is MJD type 4, which presents parkinsonian features with mild cerebellar deficits (Suite et al 1986).

1.5.3 Neuropathology and pathogenesis

MJD affects multiple systems involving neurodegeneration both in white matter of the cerebellum, spinal cord and brainstem, and gray matter of several areas, such as: 1) cerebellothalamocortical motor loop; 2) basal ganglia-thalamocortical motor loop; 3) the visual, auditory, somatosensory, oculomotor and vestibular system; 4) the ingestion-related and pre-cerebellar brainstem system; 5) the pontine noradrenergic system and the dopaminergic and cholinergic midbrain system (Rub et al 2008). In MJD patients, deficits in glucose consumption have been described in the cerebellum, brainstem, and cerebral cortex, even before any clinical signs of disease (Soong & Liu 1998).

At the molecular level, MJD is poorly understood; however, it is expected that the described neurodegeneration is a result of several events. The main difference between wild-type and mutant ataxin-3 is the higher propensity to misfold and aggregate at a faster rate due to polyQ expansion (Ellisdon et al 2006). Aggregation of mutant ataxin-3 leads to the formation of nuclear inclusions containing not only this protein but also proteins involved in proteasome system, such as: ubiquitin, molecular chaperones, transcription factors and non-expanded ataxin-3. The nuclear inclusions are found mainly in the nucleus of neuronal cells (Natalello et al 2011,

Reina et al 2010). However, similar inclusions were also reported in axons, possibly impairing axonal transport (Chai et al 1999, Seidel et al 2010).

Another theory has been developed explaining MJD neuropathology as a result of toxic fragments of mutant ataxin-3. This protein is susceptible to proteolysis, releasing a polyQ monomer which acquires β-strand conformation and enhances oligomers formation (Nagai et al 2007, Pozzi et al 2008). In fact, when mutant ataxin-3 proteolysis was inhibited, the neuronal dysfunction and neurodegeneration caused by this protein were reduced (Simoes et al 2012).

Moreover, the normal function in protein homeostasis may be affected, due to aberrant interactions of ataxin-3 with its native substrates, resulting either in gain of function or loss of its normal activity, as reviewed in (Costa Mdo & Paulson 2012). An example is the interaction with transcriptional factors favored due to the expanded ataxin-3 accumulation in the nucleus, thus deregulating transcription (Lim et al 2008). Interestingly, expanded ataxin-3 binds to chromatin in different sites and has shown to increase transcription in cells, when comparing to non-expanded ataxin-3 (Evert et al 2006, Evert et al 2003). Furthermore, transcription dysregulation caused by expanded ataxin-3 may affect apoptosis regulation, cell signaling and synaptic transmission, since in a transgenic mouse model of MJD was demonstrated messenger RNA downregulation of proteins involved in pathways, such as intracellular calcium signaling and upregulation of pro-apoptotic genes, such as Bax (Chou et al 2008).

On the other hand, loss of function may affect the proteasome system, which can disturb neuronal function (Chai et al 1999). However, since the absence of this protein in mice and *Caenorhabditis elegans* has not produced a significant neurodegenerative and ataxic phenotype, it is more consensual that neuronal toxicity in MJD is a result of expanded ataxin-3 gain of function (Schmitt et al 2007).

Autophagy is also implicated in MJD, in part due to interactions of ataxin-3 aggregates with relevant proteins involved in this mechanism, as was described in MJD models (Ashkenazi et al 2017). In fibroblasts of MJD patients, it has been demonstrated a compromised autophagic flux, which affects the degradation of cellular components (Nascimento-Ferreira et al 2011, Onofre et al 2016). Furthermore, expanded ataxin-3 has been described to deregulate the endoplasmic reticulum-associated degradation, a machinery responsible to assist the degradation of misfolded proteins. (Evers et al 2014, Laco et al 2012a).

Cellular stress in MJD also includes mitochondrial dysfunction, demonstrated both in cellular and mouse models. Such alterations are mitochondrial DNA damage, reduced energy supply, decrease in antioxidant enzymes levels, such as superoxide dismutase, and dysfunction in respiratory chain complex II (Kazachkova et al 2013, Laco et al 2012b, Yu et al 2009). Thus, in MJD, with the mitochondrial activity impaired, cells become much more susceptible to oxidative stress caused by free radicals (Evers et al 2014).

Additionally, dysregulation of Ca^{2+} homeostasis may be involved in MJD, since it has been described that mutant ataxin-3 enhances activation of an intracellular calcium channel and inhibition of calcium release produced a benefic effect in motor performance and neurodegeneration. This effect may be, in part, explained by inhibition of proteolysis of mutant ataxin-3 by the calcium-dependent calpains (Makarewicz et al 2003).

Furthermore, in a *Drosophila* model of MJD, it was demonstrated that the toxicity is not exclusive conferred by this polyQ containing protein, but also results from the corresponding RNA which recruits several proteins causing toxicity to the cells (Li et al 2008). Moreover, microRNAs and its corresponding machinery were also downregulated in both *in vitro* and *in vivo* models of MJD, which may contribute to disease pathogenesis since this deregulation was associated with aggravated phenotype in a MJD mouse model (Carmona et al 2017).

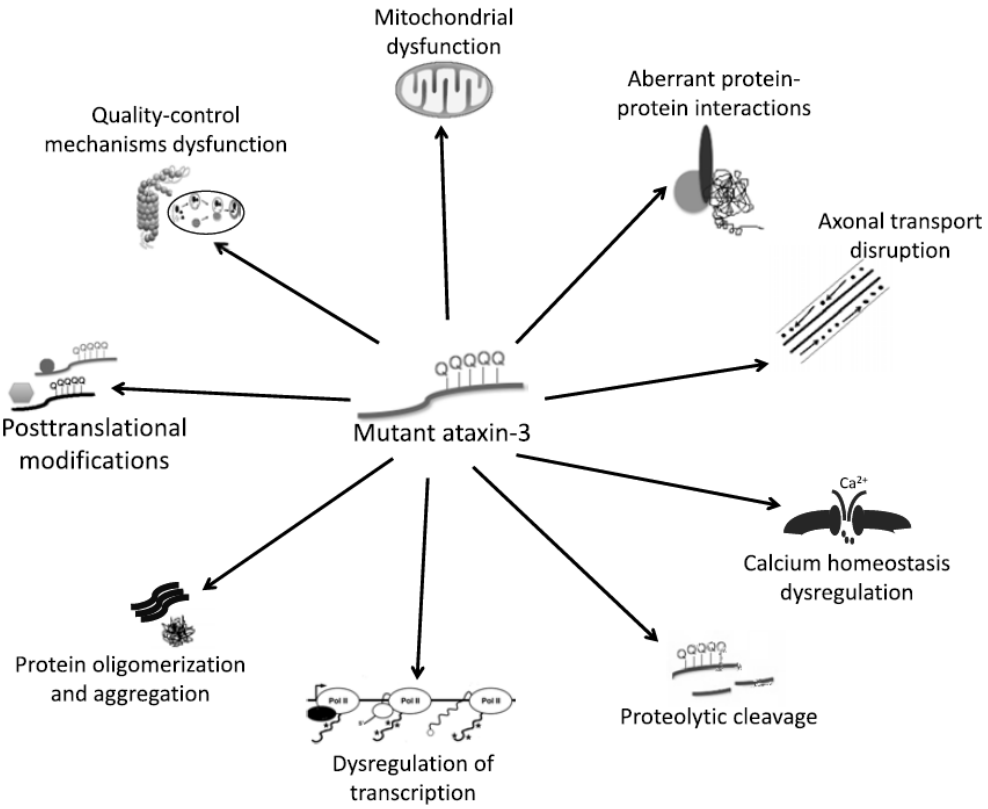

Figure 1.5. The mechanism underlying mutant ataxin-3 cellular toxicity in MJD. Mutant ataxin-3 have been associated with abnormalities in several cellular components, such as quality control systems, mitochondria, axonal transport, calcium homeostasis, transcriptional regulation, among others. Reviewed in (Nóbrega 2012).

1.5.4 Mouse models of MJD

Several animal models have been developed in mice, rats, flies and worms to mimic the principal MJD features and attempt to fully recapitulate the disease. Overexpression of specific forms of ataxin-3 in transgenic mouse models share important anatomical and molecular similarities with the disease in humans. However, models may vary in the promoter, number of CAG repeats and portions of ataxin-3, which lead to diverse forms of the disease, with differences in severity, onset time, nuclear inclusions formation and level and sites of neurodegeneration. In most mouse models, it has been used a complementary DNA sequence, encoding a particular isoform of ataxin-3, under the expression of a foreign promoter, as reviewed in (Costa Mdo & Paulson 2012). An exception is a mouse model with genomic integration of full-length human *MJD1* gene in a yeast artificial chromosome (Cemal et al 2002).

Model diversity allows the understanding of distinct mechanisms involved in MJD as well as the interactions between them. For instance, Ikeda and collaborators developed a model expressing full-length human mutant ataxin-3 under the control of the L7 promoter, which failed to reproduce neurodegeneration. In contrast, when they used the same promoter and expressed a truncated form of mutant ataxin-3 with the polyQ fragment, mice showed severe cerebellar atrophy and progressive ataxia (Ikeda et al 1996). Boy et al. generated a mouse model of MJD with rat huntingtin promoter to control mutant ataxin-3 expression in brain. This model has more similarities with MJD than the previous one, showing late onset symptoms, nuclear inclusions formation and significant neurodegeneration (Boy et al 2010).

The MJD model used in this work was produced by Torashima and collaborators and resulted in a “polyQ transgenic mice” bearing an N-terminal truncated form of human ataxin-3 with 69 CAG repeats, together with an N-terminal haemagglutinin (HA) epitope, expressed under the

control of L7 promoter, i.e. specific for Purkinje cells of the cerebellum (Torashima et al 2008). This animal model shows expression of aggregates and the severe phenotype associated starts 21 days after birth. In this model the cerebellum is mainly affected, particularly in Purkinje cells, allowing the study of disease pathogenesis in this brain region. Defects in these cells are expressed as cerebellar ataxia, the cause of impaired balance and gait disturbance shown by these MJD mice (Torashima et al 2008).

1.5.5 Can BBB be impaired in MJD?

Similarly with another neurodegenerative diseases that have been described to involve BBB dysfunction, MJD also involves neuroinflammation. In fact, neuroinflammation is a well-known participant in neurodegeneration (Cardoso et al 2015). Increased immune response in MJD brains has been revealed by the increased expression in interleukin 6 and 1 and markers for reactive microglia (ionized calcium-binding adapter molecule 1) and astrocytes (glial fibrillary acid protein) (Evert et al 2001, Rochfort & Cummins 2015). In addition, it is expected that MMP activity is deregulated as an effect of neuroinflammation. In fact, mutant ataxin-3 is known to modify the expression of MMP-2 (Evert et al 2006). In the other neurodegenerative diseases described above, neurovascular unit was also affected by a deficient neurovascular coupling due to neurodegeneration and alterations in astrocytes and microglia proliferation (Thiollier et al 2016). Thus, as MJD involves neurodegeneration, neuroinflammation and consequent MMPs dysregulation, it is expected that vascular alterations and BBB dysfunction are also contributing to MJD neuropathology.

1.6 Objectives

The aim of this work was to evaluate the cerebrovascular and CNS-barriers integrity in MJD.

To accomplish that, two experiments were performed. In the first experiment of this work, we assessed BBB permeability by quantifying the Evans blue (EB) extravasation in the brain of a transgenic mouse model of MJD, as compared to age-matched wild-type littermates.

Having evidences of BBB impairment in the cerebellum of the MJD model used in this study, in the second experiment, we aimed to assess which mechanisms were involved in BBB disruption. Thus, in the cerebellum of transgenic and wild type, we investigated: the presence of mutant ataxin-3 aggregates in cerebellar blood vessels, the density of these vessels, fibrin extravasation across BBB, and the expression TJ-associated proteins in both BBB and BCSFB. Finally, perfusion and vascular permeability were evaluated by Dynamic Contrast Enhanced-Magnetic Resonance Imaging (DCE-MRI) analysis.

2. Materials and Methods

2.1 Animals

A poly Q69-transgenic MJD mouse model was used in this study (Torashima et al 2008). This animal model has a C57BL/6 background and express a truncated form of human ataxin-3 with 69 CAG repeats, which lacks the 286 N-terminal aminoacid residues and it is preceded by the HA epitope. The transgene expression is driven by the L7 promoter, which restricts ataxin-3 expression to the Purkinje cells localized in the cerebellum. As a consequence of mutant ataxin-3 accumulation in the cerebellum, polyQ69-transgenic mice show severe cerebellar atrophy and ataxic symptoms, already manifested at postnatal day 21. A colony of this transgenic mouse model was established at Center for Neuroscience and Cell Biology of the University of Coimbra. The colony was maintained in our lab by backcrossing C57BL/6 females with heterozygous males. Transgenic mice and age-matched wild type animals were housed in a temperature-controlled room on a 12h light/12h dark cycle with food and water provided *ad libitum.* Genotyping was performed by Polymerase Chain Reaction at 4 weeks of age.

All the animal experiments were carried out in accordance with the European Community Council Directive (86/609/EEC) for the care and use of laboratory animals and previously approved by the Responsible Organization for the Animals Welfare of the Faculty of Medicine and Center for Neuroscience and Cell Biology of the University of Coimbra (ORBEA and FMUC/CNC, Coimbra, Portugal).

The present study was divided in two experiments. In the “Experiment 1”, four polyQ69-transgenic MJD mice and six wild type littermates with 11 months old were used; in the “Experiment 2”, seven polyQ69-transgenic MJD mice and nine wild-type mice with 17 months old were used.

2.2 EXPERIMENT 1:

2.2.1 Evans blue (EB) injection, Sacrifice and Tissue collection

Eleven-month old mice were injected with 2% EB (100µL/30g) in the caudal vein. After 30 minutes, animals were sacrificed by transcardial perfusion with phosphate buffered saline 1x (PBS) solution followed by brain and liver dissection. Brain hemispheres were divided for fluorescence microscopy (left hemisphere) and spectrophotometric analysis (right hemisphere; cerebellum and cerebrum were analyzed separately). Schematic timeline in Figure 3.1.

2.2.2 EB quantification by spectrophotometry

The liver and the right hemisphere of the brain were incubated overnight with 6 times the volume of its weight of pure formamide, in a water bath at 70ºC with permanent agitation. Subsequently, the organs were centrifuged at maximum speed, at 4ºC, and the supernatant absorbance was measured at 620 nm and 720 nm using the light detector Fluorimeter SpectraMax Gemini EM (Molecular Devices). Absorbance values at 620 nm were subtracted to absorbance values at 720 nm and compared with a pre-defined standard curve. Finally, brain values were normalized with liver EB quantity to exclude variances during EB injection.

2.2.3 EB detection by fluorescence microscopy

The left hemisphere was sliced in 35µm sagittal sections with a cryostat (Leica CM3050S) at −20°C and placed directly onto superfrost microscope slides (Thermo Scientific). Fluorescence microscopy analysis was performed in brain sections with lateral coordinates between 0.84mm to 0.12mm (from figure 101 to 108, as described in the mouse brain atlas (Franklin & Paxinos 2001). For that, brain sections were hydrated with PBS 1X during 30 minutes, followed by nuclear staining with DAPI (4',6-diamidino-2-phenylindole) and coverslipped on Dako fluorescence mounting medium. Images were acquired with Zeiss Axio Imager Z2 microscope (Carl Zeiss Microimaging), equipped with a High Resolution Monochromatic Camera and with Plan-Apochromat 20X/0.8 M27 objective.

2.3 EXPERIMENT 2

2.3.1 Sacrifice and Cerebellum dissection

Seventeen-month-old mice (7 transgenic and 9 wild type) were anaesthetized via intraperitoneal route and transcardially perfused with cold PBS 1X, pH 7.4. Perfused cerebella were dissected, left part was preserved in tissue tek (Sakura) and cut in 35µm sagittal sections in a cryostat (Leica CM3050S) at −20°C and placed directly onto superfrost microscope slides (Thermo scientific). Slides were stored at -20ºC until further processing. The right half of the cerebellum was stored at -80ºC for further protein extraction. See schematic timeline of experiment 2 in Figure 3.2.

2.3.2 Immunofluorescence

Sections previously placed on superfrost slides were hydrated with PBS 1X during 30 minutes, followed by incubation with blocking/permeabilization solution of 3% bovine serum albumin (BSA) with 0.1% Triton X-100) during 1 hour at room temperature. Then, sections were incubated 48h at 4ºC with the respective primary antibodies diluted in 0.3% BSA: goat anti-CoIV (1:250, #AB769 Millipore), mouse anti-HA (1:500, #MMS-101P BioLegend) and rabbit anti-Fibrin/FITC (1:40, #F011102-2 Dako). Double immunofluorescence was performed for the following combinations: ataxin-3 aggregates (HA) with CoIV, and fibrin with CoIV. Afterwards, sections were incubated with the respective secondary antibody, anti-goat Alexa Fluor 568 (1:200, #A11057 Life Technologies) or anti-mouse Alexa Fluor 488 (1:200, #A-11001 Life Technologies) diluted in PBS 1X, during 2 hours at room temperature, before nuclear staining with DAPI. Finally, slides were coverslipped on Dako fluorescence mounting medium (S3023) and stored at -20ºC.

2.3.3 Immunofluorescence quantitative analysis

Co-localization of ataxin-3 aggregates with CoIV-positive blood vessels

Cerebellum images were acquired with a Zeiss Axio Imager Z2 microscope (Carl Zeiss Microimaging), equipped with a High Resolution Monochromatic Camera and the Plan-Apochromat 40X/1.3 M27 objective. One section per animal corresponding to the same cerebellar region was used to analyze immunofluorescence. Evaluation of the presence of ataxin-3

aggregates (HA staining) within CoIV-positive blood vessels was performed in serial Z-stacks of cerebellum using Zen software (Zeiss).

Quantification of CoIV-positive area in the cerebellum

Images created by acquiring tiles of the entire cerebellum with Plan-Apochromat 20X/0.8 M27 objective were analyzed using Image J software (National Institutes of Health; http://imagej.nih.gov/ij). One section per animal corresponding to the same cerebellar region was used to analyze immunofluorescence. The same threshold for fluorescence intensity was applied to all images and the percentage of surface area positive for CoIV staining in the cerebellum was measured.

Quantification of Extravascular Fibrin

Extravascular fibrin in the cerebellum was quantified by measuring the percentage of surface area positive for fibrin staining outside blood vessels, as previously described by Drouin-Ouellet et. al (Drouin-Ouellet et al 2015). Briefly, one similar cerebellar region per animal was incubated with primary antibodies against CoIV and fibrin. After image acquisition with Plan-Apochromat 20X/0.8 M27 objective in Zeiss Axio Imager Z2 microscope, a magenta mask for CoIV and a yellow mask for fibrin staining were obtained with Image J. The masks were then merged in Adobe Photoshop (Adobe Systems Incorporated) showing the co-localization of CoIV and fibrin, which appeared in white (resulting from the merge of magenta and yellow). After removing magenta and white from the image, leaving only extravascular fibrin staining, the percentage of surface area was measured using Image J (Figure 2.1).

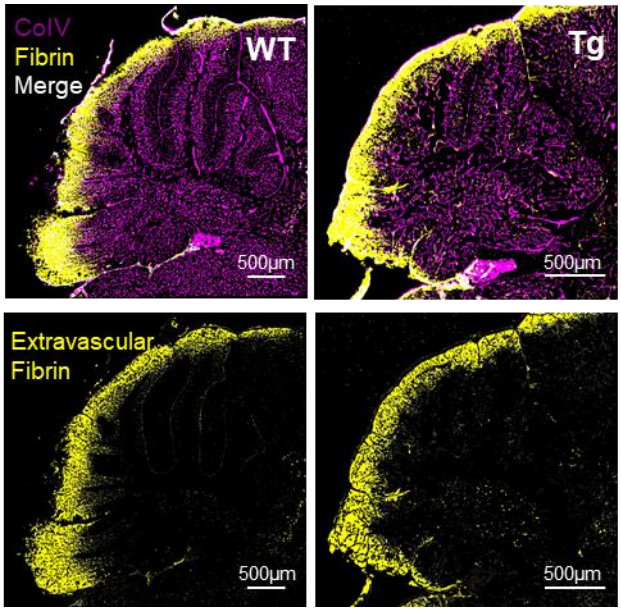

Figure 2.1. Representative example of quantification of extravascular fibrin. Collagen IV (CoIV) and fibrin stainig were converted into magenta and yellow masks , respectively, with Image J for transgenic (Tg) and wild-type (WT) littermates. Masks merge in Adobe Photoshop showed the co-localization of CoIV and fibrin in white (resulting from the merge of magenta and yellow). Extravascular fibrin was obtained by removing magenta and white from the image.

2.3.4 Protein Extraction and Western blotting

The right side of the cerebellum was firstly homogenized with Ambion TRIzol reagent (Fisher Scientific) and then subjected to density gradient with chloroform to remove the RNA

aqueous phase. DNA was precipitated with 100% ethanol, leaving the protein in the phenol-ethanol phase. Isopropanol was added to precipitate protein, which was pelleted and washed with guanidine-ethanol solution and 100% ethanol. Dried pellet was then solubilized in urea/Dithiothreitol solution with protease inhibitors (Roche Diagnostics), followed by incubation at 95ºC during 5 minutes. Total protein extracts were stored at -80ºC.

Bradford protein assay (BioRad) was used to determine protein concentration. Thirty to forty micrograms of protein extract were resolved on sodium dodecyl sulfate-polyacrylamide gels (4% stacking and 10% running). Proteins were then transferred onto a polyvinylidene difluoride membrane (Millipore), previously blocked with 5% non-fat milk powder dissolved in 0.1% Tween 20 in Tris-buffered saline for 1 hour at room temperature. Membranes were then incubated overnight at 4°C with primary antibodies: anti-ZO-1 (1:100, #61-7300 Life Technologies), anti-claudin 5 (1:250, #34-1600 Life Technologies) and anti-occludin (1:100, #71-1500 Life Technologies). The correspondent alkaline phosphatase-linked goat anti-mouse or anti-rabbit secondary antibodies were incubated for 2 hours at room temperature. Bands were detected after incubation with Enhanced Chemifluorescence Substrate (GE Healthcare) and visualized in chemifluorescence imaging (ChemiDocTM Touch Imaging System, Bio-Rad Laboratories). Semi-quantitative analysis was carried out based on the bands of scanned membranes using Image J (National Institutes of Health) and normalized with respect to the amount of β-tubulin loaded in the corresponding lane of the same gel.

2.3.5 Dynamic Contrast-Enhanced-Magnetic Resonance Imaging (DCE-MRI)

Acquisitions of *in vivo* images were conducted with a 9.4 T magnetic resonance small animal scanner BioSpec 94/20, with a standard Bruker cross coil setup using a volume coil for excitation (with 86/112 mm of inner/outer diameter, respectively) and quadrature mouse surface coil for signal detection (Bruker Biospin, Ettlingen). Experiments were performed at the Institute for Nuclear Sciences Applied to Health, University of Coimbra. Animals were anesthetized with isoflurane (1–2%) (delivered through the system E-Z SA800, Euthanex, Palmer), with constant temperature monitoring (Haake SC 100, Thermo Scientific) and assessment of cardiorespiratory function (1030, SA Instruments Inc., NY).

Dynamic contrast-enhanced images were acquired with a fat-saturated T1-weighted gradient-echo sequence with parameters: TR/TE = 251.446/2.5 ms, FA = 70°, FOV = 20×20 mm2, matrix size = 108×71, 24 slices (coronal orientation), slice thickness = 0.5 mm, 40 dynamics, 7 averages, scan time per dynamic = 125 s, total scan time = 1hour and 23 minutes. The gadolinium-based contrast agent named Gadobutrol (Gadovist®, LUSAL) was administered intraperitoneally, after the acquisition of 8 baseline dynamics.

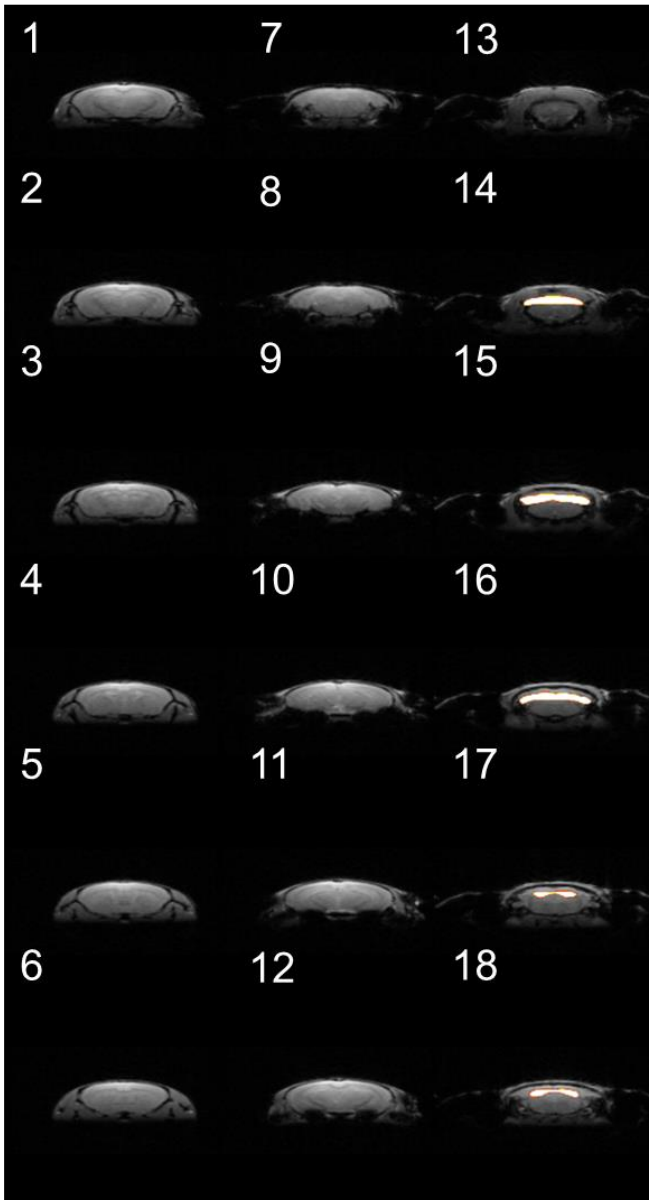

Figure 2.2. **Coronal T1-weighted anatomical MRI sequence of the defined ROI in the cerebellum of mice**. Eighteen sequential slices with 0.5 mm of thickness were acquired to select the cerebellum as ROI (here colored in white) by a semiautomatic procedure.

In perfusion analysis, data were analyzed offline using homemade software implemented in Matlab (v2013a, Mathworks, Natick) to obtain tissue/contrast enhancement curves. A Region of interest (ROI) was drawn for each animal corresponding to the cerebellum, as shown in Figure 2.2, in separate using a semiautomatic procedure. The mean variation of signal intensity, or cerebellum enhancement curve, as a function of time was then quantified in the predefined ROI. Mean area under the curve (AUC) was calculated to evaluate perfusion and vascular permeability. Typical tissue enhancement curve is summarized in Figure 2.3. Briefly, after contrast agent administration, the curve reproduces a rapid rise in tissue enhancement due to contrast agent entry in capillary network, indicating the cerebellum blood flow (Figure 2.3-1). The first peak of the curve corresponds to the maximum contrast agent quantity to reach the cerebellum, which provides information about the cerebellum blood volume (Figure 2.3-2). As contrast agent recirculates in the capillaries, it accumulates in the tissue interstitium depending on capillaries permeability and surface product (Figure 2.3-3). The last part of the curve represents

the elimination of the contrast agent by renal filtration. The kinetics of elimination depends on the interstitial volume of the cerebellum, in this case (Figure 2.3-4).

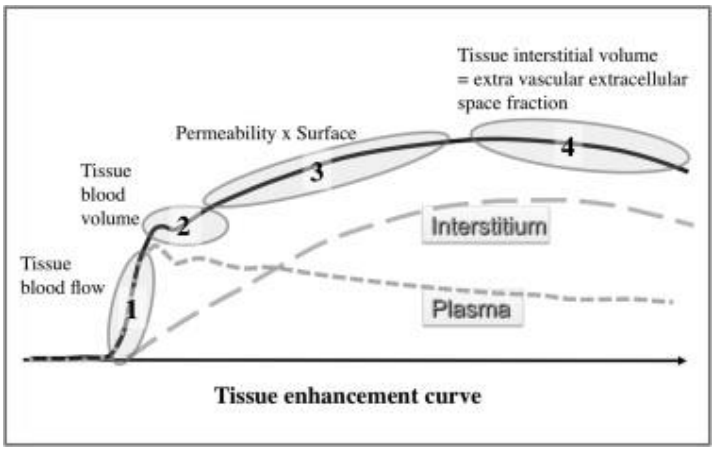

Figure 2.3. Schematic interpretation of tissue enhancement curve produced by dynamic contrast enhanced-magnetic resonance imaging (DCE-MRI) technique with the injection of contrast agent. The continuous curve is the sum of tissue enhancement produced by the contrast agent in the plasma (grey large lines) and in the interstitium (grey small lines). The different parts of the curve give information about different aspects of the vasculature being analyzed. The slope of the first part (1) is an indicator of the tissue blood flow; the first peak (2) corresponds to the tissue blood volume; the permeability of the blood vessels is indicated by the slope corresponding to 3 and the last part (4) refers to the interstitial volume of the tissue. Adapted from (Cuenod & Balvay 2013).

2.4 Statistical Analysis

GraphPad Prism software was used to present data as mean ± standard error of mean (SEM) and outliers were removed according to Grubb's test (alpha=0.05). Unpaired t-test was performed to compare wild type and transgenic groups. Significance was determined according to the following criteria: p>0.05= not significant; *p≤0.05, **p<0.01 ***p<0.001 and ****p< 0.0001.

3. Results

In the present work, we aimed to study the BBB integrity and cerebrovascular network in MJD. To achieve that, in the first experiment of this work, we assessed BBB permeability by quantifying the EB extravasation in the brain of a transgenic mouse model of MJD, as compared to age-matched wild-type littermates. In the second part, we aimed at understanding the mechanisms involved in the observed BBB disruption, investigating mutant ataxin-3 presence in cerebellar blood vessels, and its impact on vascular changes in the cerebellum. Finally, perfusion and vascular permeability were evaluated by DCE-MRI analysis with administration of a contrast agent.

3.1. EB extravasation in the cerebellum of MJD transgenic mice

EB dye is known to strongly bind to albumin and it has been widely used to evaluate BBB permeability in many neuropathologies, since it is not able to cross the brain endothelium when BBB integrity is maintained (Rössner & Tempel 1966). Having this in mind, in our first experiment (see schematic presentation in Figure 3.1 A), eleven-month-old mice were injected with EB (2%) in the caudal vein and sacrificed 30 minutes later. After that, the left hemisphere of the brain was used for fluorescence analysis, while the right hemisphere was separated into cerebrum and cerebellum and, together with the liver, was used for EB quantification by spectrophotometry. At the end, EB concentrations in cerebrum and cerebellum were normalized with liver EB concentrations, in order to exclude variations caused by differences in the amount of EB injected.

As shown in Figure 3.1 B, no significant differences were observed in the levels of EB in the cerebrum of transgenic mice, as compared to wild type littermates; likewise, upon normalization with EB concentration in the liver, no differences were found between these two groups (Figure 3.1 D). On the contrary, a significant increase of EB was observed in the cerebellum of transgenic mice (approximately 5 fold increase, $p=0.001$, Figure 3.1 C). A similar result was obtained when EB concentration was normalized with liver concentrations; in this case, of approximately 6 fold increase ($p=0.0007$, Figure 3.1 E).

Fluorescence microscopy images confirmed this result, since EB was more abundant in the cerebellum of MJD mice, as compared to age-matched control subjects (Figure 3.1 F). As shown, EB staining reveals vascular leakage, predominantly, in deep cerebellar nuclei (DCN) and lobules 8, 9 and 10.

Overall, these findings indicate that BBB is disrupted in the cerebellum of this transgenic animal model of MJD.

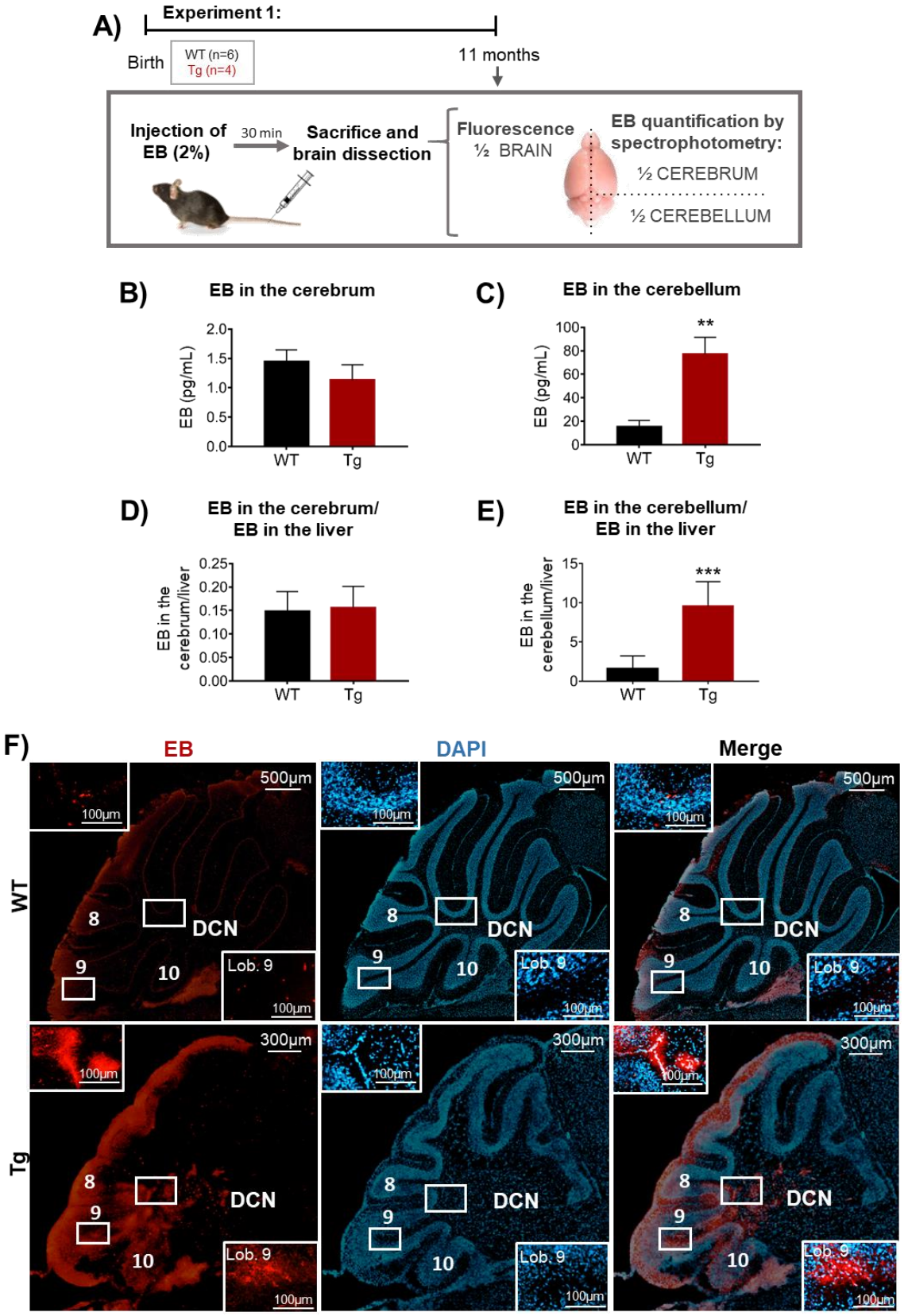

Figure 3.1 – Evans blue (EB) extravasation in the cerebellum of MJD transgenic mice suggests BBB disruption (see legend in the next page).

Legend of Figure 3.1: A) Schematic presentation of Experiment 1. Four MJD transgenic (Tg) and 6 wild type (WT) animals with 11 month-old were injected with 2% Evans blue (EB) into the tail vein. After sacrifice, brain and liver were dissected and EB concentration was measured by spectrophotometry and seen by immunofluorescence. B-E) EB quantification in the cerebrum and cerebellum by spectrophotometry analysis: EB concentration in the cerebrum showed no differences between wild type and transgenic animals (B). Cerebellum, on the other hand, presented higher levels of EB in MJD transgenic mice (C). These differences were maintained when EB concentrations were normalized with liver concentrations (D and E, respectively). F) Representative fluorescence images of 35µm sections of the cerebellum of wild type and transgenic mice showed EB deposition mainly in deep cerebellar nuclei (DCN) and lobule 9 of transgenic animals. Images were acquired using a microscope Axio Imager Z2 (Zeiss) with 20x objective. Values are presented as mean ± SEM. Unpaired t-test, $p>0.05$= not significant; $^{**}p<0.01$ and $^{***}p<0.001$.

3.2. Unraveling the mechanisms of BBB disruption in the cerebellum of a MJD transgenic mouse model

Having evidences of BBB impairment in the cerebellum of the MJD model used in this study, next we aimed to assess which mechanisms were involved in this process. To achieve that, the cerebellum of 17-month-old mice (7 transgenic and 9 wild type), were evaluated for: i) the presence of mutant ataxin-3 aggregates in cerebellar blood vessels; ii) the density of these vessels; iii) fibrin extravasation through vasculature; and iv) the expression TJ-associated proteins (see schematic presentation of experiment 2 in Figure 3.2 A).

3.2.1 Localization of ataxin-3 aggregates within cerebellar blood vessels in MJD transgenic mice.

Since the presence of mutant ataxin-3 aggregates is one important hallmark of MJD, we first evaluated if these aggregates were within cerebellar blood vessels (Paulson et al 1997). To assess that, we performed a co-immunofluorescence assay against HA, the epitope present in the transgene codifying expanded ataxin-3, and CoIV, a protein of endothelial basement membrane and a commonly used marker of blood vessels.

As shown in Figure 3.2 B, there was a co-localization of mutant ataxin-3 aggregates (HA staining) with CoIV-positive blood vessels. In accordance with the EB results from the immunofluorescence studies previously shown (Figure 3.1 F), the co-localization of mutant ataxin-3 aggregates with cerebellar blood vessels was particularly frequent in DCN (Figure 3.2 C), as well as in lobule 9 (Figure 3.2 D) of transgenic mice.

This result identified for the first time the presence of mutant ataxin-3 aggregates in cerebellar blood vessels in MJD mice.

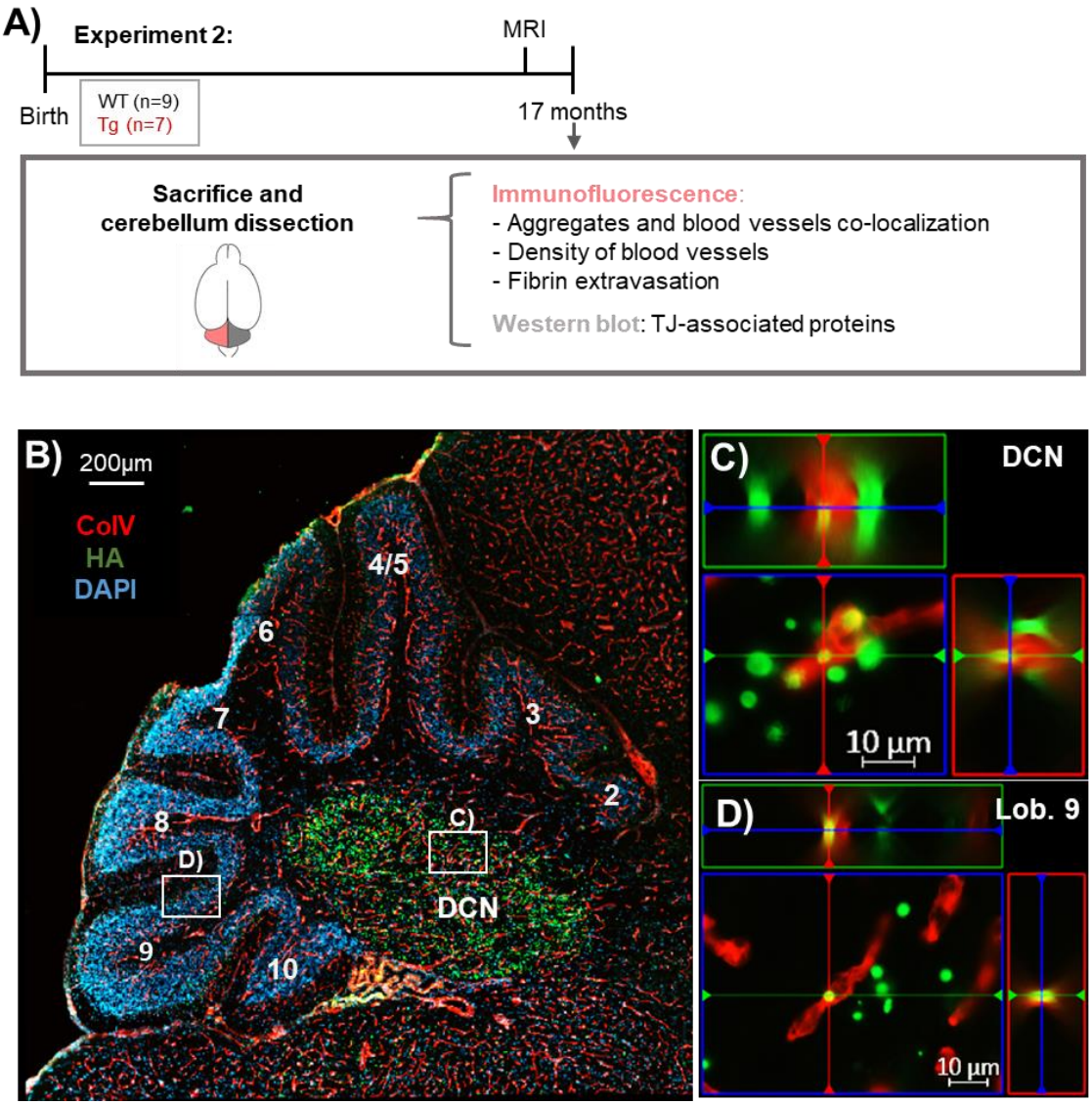

Figure 3.2 – Localization of mutant ataxin-3 aggregates within cerebellar blood vessels of MJD transgenic mice. A) Schematic representation of experiment 2, which aimed to evaluate mechanisms involved in BBB disruption in the cerebellum of MJD transgenic (Tg) mice and wild-type (WT) littermates. B) Representative co-immunofluorescence for mutant ataxin-3 aggregates (HA= hemagglutinin in green) and collagen IV (CoIV, in red) confirmed the presence of mutant ataxin-3 aggregates within CoIV-positive cerebellar blood vessels. Cerebellar lobules were identified in the image. Ataxin-3 aggregates represented in C and D were found in blood vessels of deep cerebellar nuclei (DCN) and of lobule 9, respectively, seen by the yellow color (sobreposition of red and green colors). Images were acquired using a microscope Axio Imager Z2 (Zeiss) with 20x (B) and 40x (C and D) objectives and analyzed with Zen software (Zeiss). Legenda MRI ? DAPI?

3.2.2 Global alterations in the cerebellar vasculature of MJD mice

Given that mutant ataxin-3 aggregates were detected in cerebellar blood vessels, we next investigated whether they can affect vascular morphology and functionality.

To accomplish that, we first performed an immunofluorescence staining against CoIV. Images of the whole cerebellum were acquired (Figure 3.3 A) and further analyzed with Image J

software, as previously described in Material and Methods (Chapter 2). Quantification of the percentage of surface area positive for CoIV reflected the density of blood vessels in the entire cerebellum of transgenic and wild type mice.

As depicted in Figure 3.3 B, CoIV staining revealed a significant increase in the density of cerebellar blood vessels in MJD transgenic mice (approximately 6%), as compared to wild-type littermates (p=0.03).

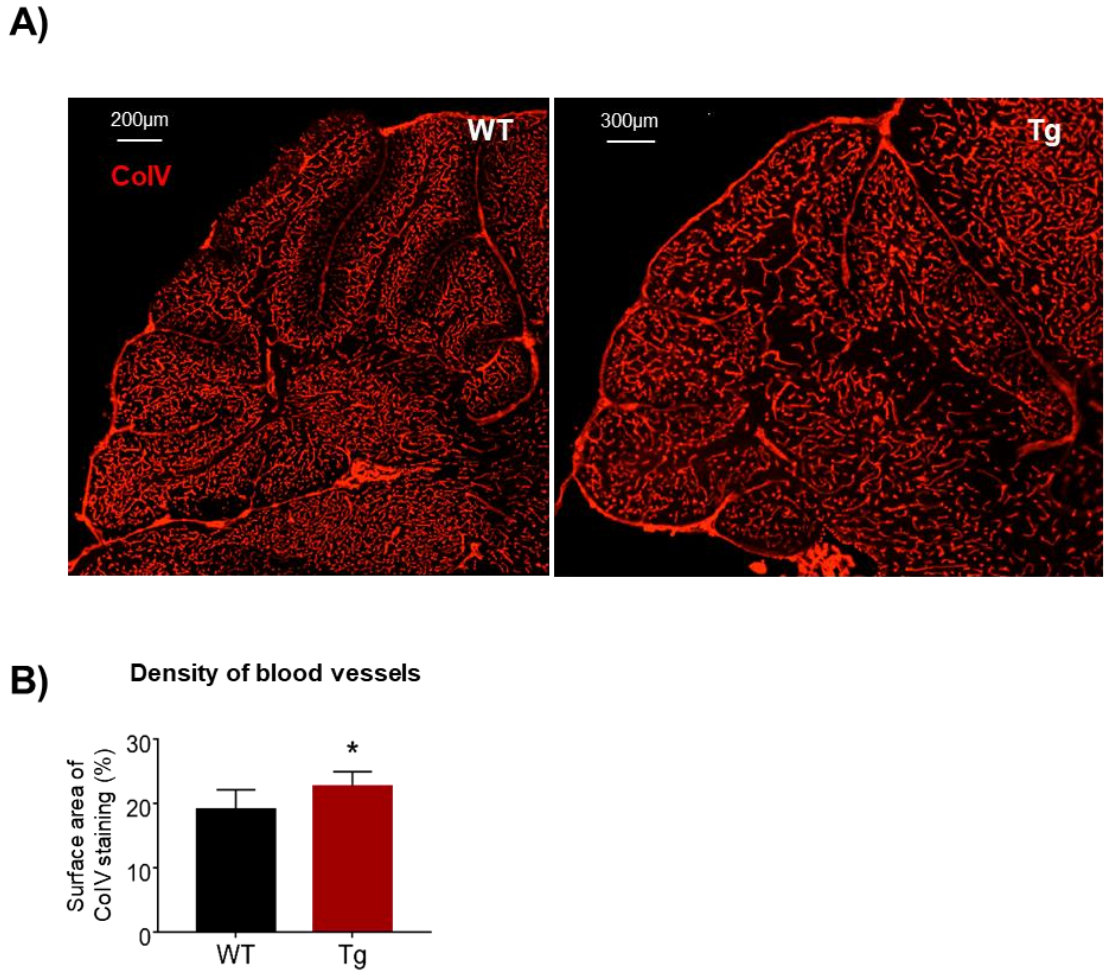

Figure 3.3 – Global alterations in the cerebellar vasculature of MJD transgenic mice. A) Representative collagen (CoIV) immunofluorescence staining, in red, performed in 35µm sections of the cerebellum of wild type (WT) and MJD transgenic (Tg) mice. B) Percentage of CoIV-positive surface area in the cerebellum of transgenic mice was significantly higher as compared to wild type, providing evidence for increased blood vessel density. Images of one section per animal were acquired using the microscope Axio Imager Z2 (Zeiss) with 20x objective and measured using Image J. Values of 6 transgenic and 9 wild type animals are presented as mean ± SEM. Unpaired t-test, * p≤0.05.

3.2.3 Fibrin extravasation in the cerebellum of MJD transgenic mice

Next we aimed to confirm whether the morphological changes seen in cerebellar blood vessels of MJD were associated with functional impairments of the BBB. For that, we measured the levels of extravascular fibrin, a blood-borne protein that crosses the BBB in higher levels when this barrier is compromised, like albumin (Yates et al 2017).

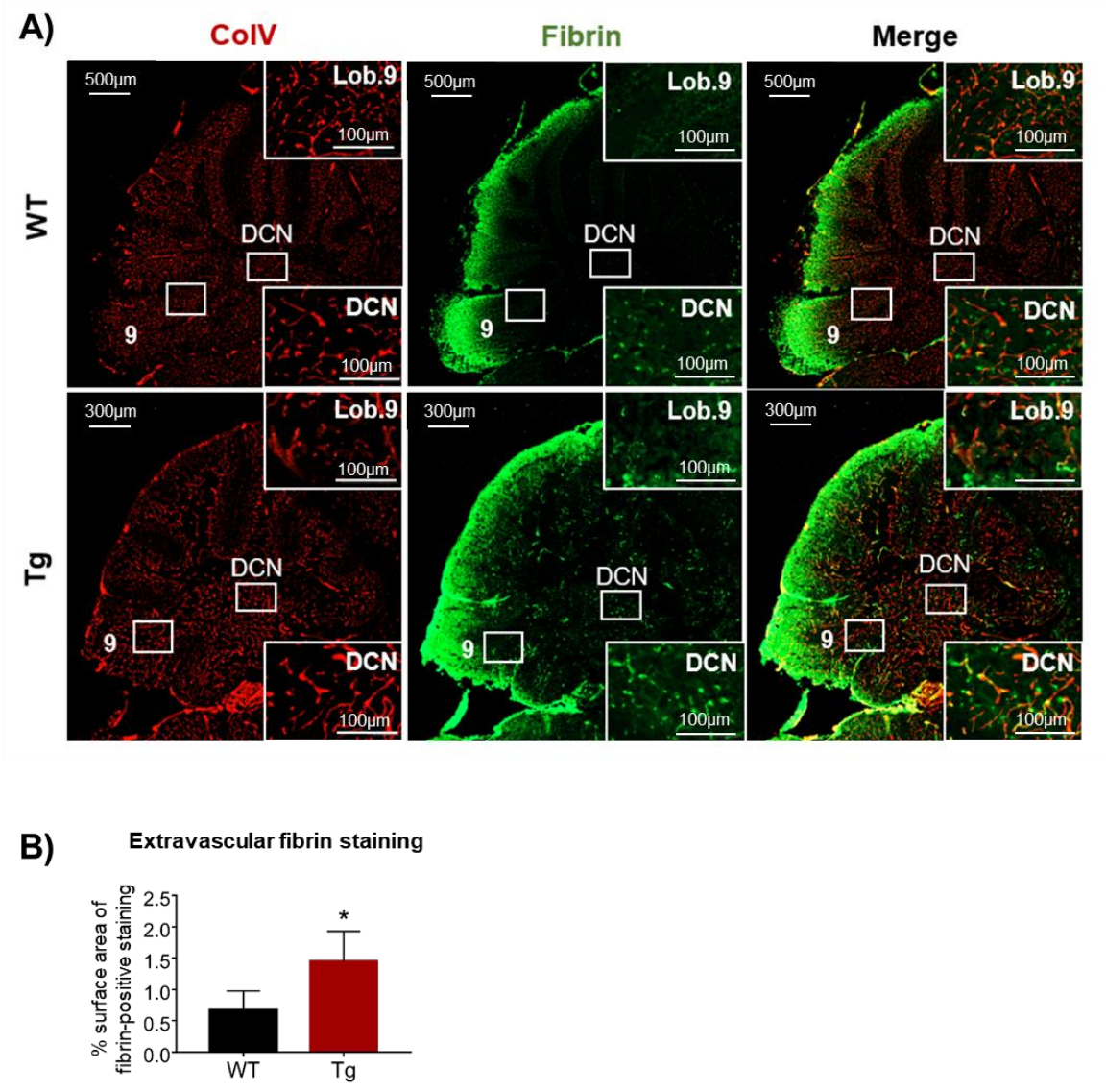

Figure 3.4 – Fibrin extravascular deposition in the cerebellum of MJD mice. A) Representative co-immunofluorescence of fibrin in green and collagen IV (CoIV) in red in the cerebellum of wild type (WT) and MJD transgenic (Tg) mice. Fibrin extravasation was more abundant in transgenic mice, particularly in deep cerebellar nuclei (DCN) and lobule 9, as shown in details. B) Extravascular fibrin was quantified according to the protocol described in Material and Methods. As shown, extravascular fibrin deposition was significantly higher in transgenic than in wild type mice. Images were acquired using Axio Imager Z2 (Zeiss). Values of 3 transgenic and 4 wild-type animals are presented as mean ± SEM. Unpaired t-test, * p≤0.05.

For that, extravascular fibrin was assessed by co-immunofluorescence against fibrin and CoIV and subsequently analyzed using Image J and Adobe Photoshop software, as described in Material and Methods (Chapter 2). As described in Figure 3.4 A, fibrin extravasation was visible in the whole cerebellum of MJD transgenic mice, being however more abundant in DCN and lobule 9.

Overall, it was observed an approximately 2-fold increase ($p=0.04$) in the extravascular fibrin deposition in the cerebellum of MJD transgenic mice, when compared to wild-type animals.

In conclusion, these results support the data from experiment 1, showing that the BBB is compromised in MJD allowing blood-borne proteins, namely albumin and fibrin, to access the cerebellar parenchyma.

3.2.4 Altered expression of TJ-associated proteins in the cerebellum of MJD mice

One of the main features of CNS-barriers (BBB and BCSFB), is the TJs formation between adjacent endothelial and epithelial cells responsible for limiting paracellular permeability (see Figure 3.5 A). As herein referred, TJ complex is constituted by transmembrane adhesion proteins, such as claudin-5 (only in the BBB), occludin, and cytoplasmic proteins, such as ZO-1, which attach the adhesion proteins to the actin cytoskeleton (Vorbrodt & Dobrogowska 2004). Taking into account ZO-1 isoforms separately, isoform α- is restricted to the endothelium, thus present in BBB, while isoform α+ is found in most epithelial-cell junctions, including choroid plexus that create BCSFB (Willott et al 1992).

In order to elucidate the mechanisms underlying CNS-barriers permeability in the transgenic mouse model used in this study, protein extracts of the cerebellum of 17-month-old mice were analyzed by Western blotting for the following TJ-associated proteins: Claudin-5, Occludin and ZO-1 (Figure 3.5 B).

Western blot analysis revealed no significant differences in Occludin relative levels, a protein found in both CNS-barriers, BBB and BCSFB (Figure 3.5 F). However, a band corresponding to an Occludin fragment with 55 kDa was observed in MJD mice and barely seen in wild-type animals (see WB, Figure 3.5 B). As described in Figure 3.5 G, its relative levels were significantly higher in transgenic animals ($p< 0.0001$). On the other hand, Claudin-5, a protein which is exclusively expressed in BBB, showed approximately a 2-fold increase in MJD transgenic mice ($p=0.005$) when compared to wild-type animals (Figure 3.5 H).

Total ZO-1 protein, including both isoforms ZO-1 α- and α+, showed no significant differences in its relative levels of expression (Figure 3.5 C). However, examining ZO-1 isoforms separately, we observed that ZO-1 isoform α+ expression shows a tendency ($p=0.08$) to decrease in transgenic animals (Figure 3.5 D), while no significant differences were found in ZO-1 isoform α- expression (Figure 3.5 E). These results suggest that ZO-1 protein expression in BBB is not affected in MJD mice, while in BCSFB the TJ assembly may be compromised, as ZO-1 isoform α+ showed a tendency to be reduced in this mouse model.

Overall, Western blotting results demonstrate that there are significant differences in the expression of TJ-associated proteins in the cerebellum of MJD mice, particularly the cleavage of Occludin and the increase in the levels of Claudin-5. Moreover, ZO-1 isoform α+, which is present in BCSFB, shows a tendency to decrease in transgenic animals. Taken together, these findings suggest both CNS-barriers (BBB and BCSFB) are probably compromised due to TJ-associated proteins alterations.

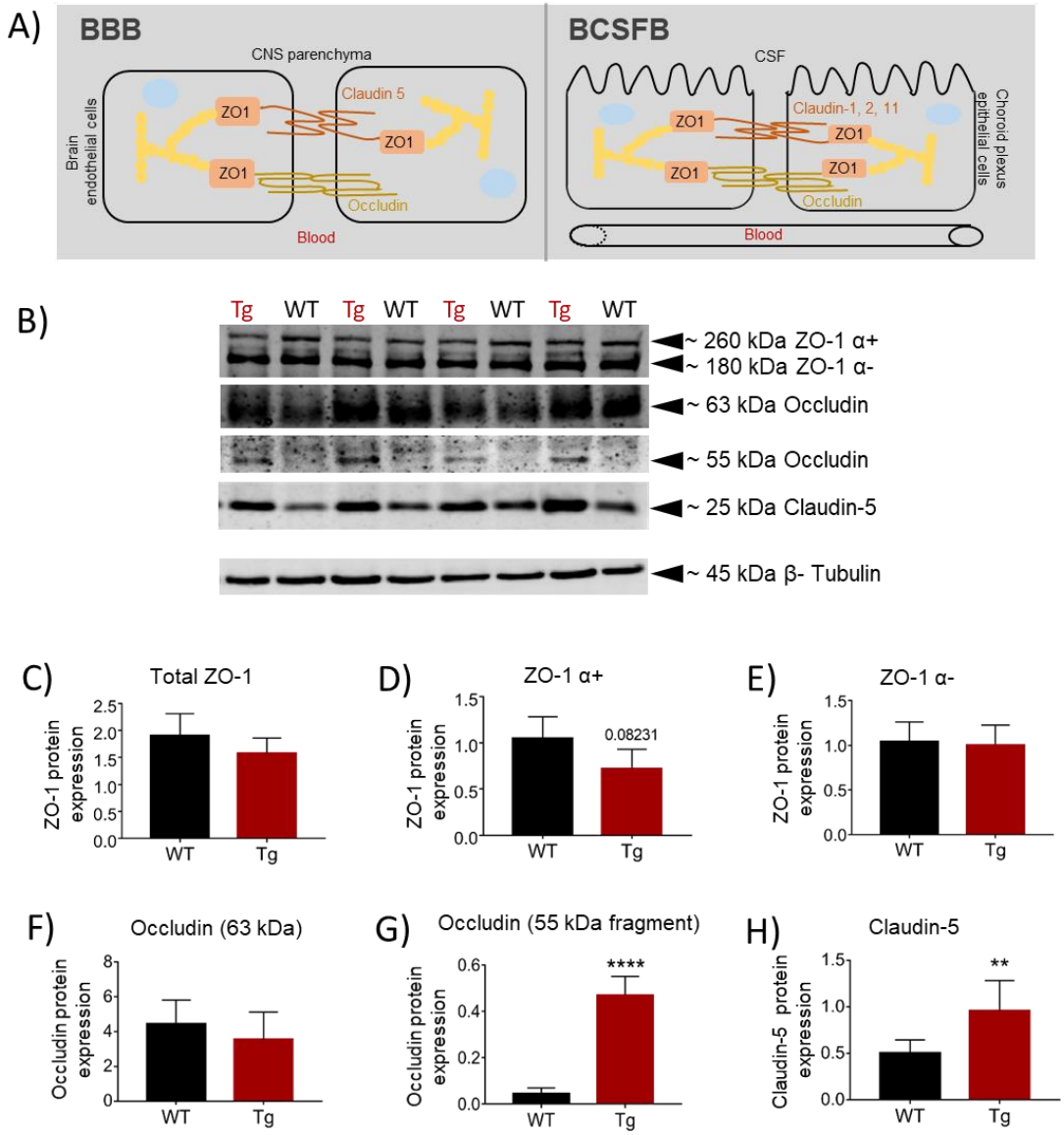

Figure 3.5 – Expression levels of tight junction (TJ)-associated proteins in the cerebellum of MJD mice differ from wild-type controls. A) Schematic representation of TJ structure in central nervous system (CNS)-barriers, both blood-brain barrier (BBB) and blood-cerebrospinal fluid barrier (BCSFB). B) Representative western blot membrane of TJ-associated proteins in the cerebellum of transgenic (Tg) and wild type (WT) mice. C-H) Western blot quantification of TJ-associated proteins. C-E) Relative levels of total zonula occludens-1 (ZO-1) (C), ZO-1 α+ isoform (D), ZO-1 α- isoform (E) showed no significant differences between transgenic (n=4) and 4 wild type (n=4) mice. F, G) Relative levels of Occludin (63 kDa) (F) were similar in the two groups, but the 55kDa occludin fragment (G) was strongly presented in the cerebellum of transgenic mice (n= 6), when compared to wild type mice (n=7). H) TJ-associated protein Claudin-5 was significantly increased in transgenic (n=7) relatively to wild type mice (n=7). All protein relative levels were normalized with β-tubulin. Values are presented as mean ± SEM. Unpaired t-test, $p>0.05$= not significant; $^{**}p<0.01$ and $^{***}p<0.001$.Legenda kDa ?

3.2.5 In vivo evidence of CNS-barriers disruption using DCE-MRI

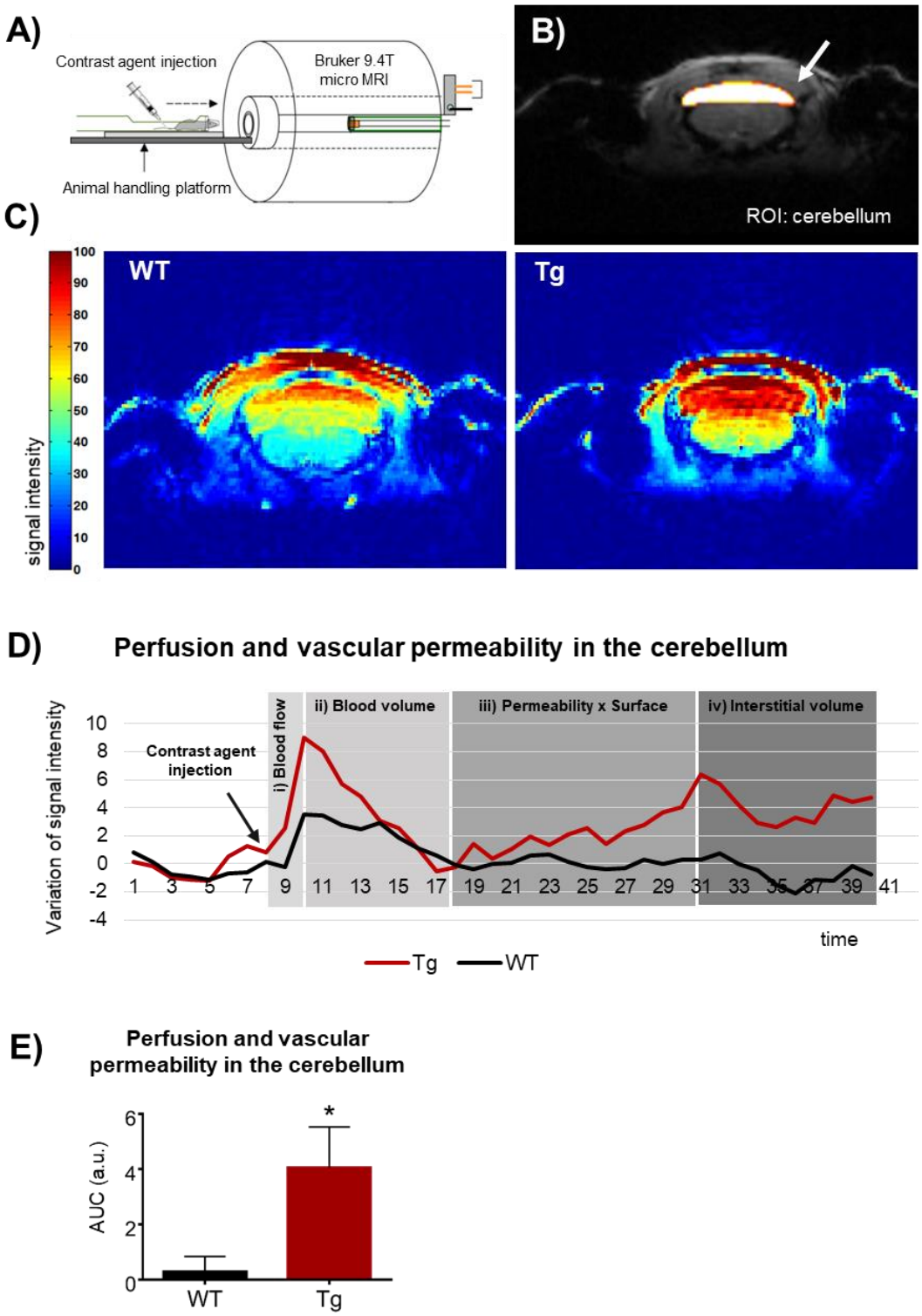

Figure 3.6 – *in vivo* evidence of alterations in the perfusion and vascular permeability with consequent contrast agent accumulation in the cerebellum of MJD transgenic mice using DCE-MRI. (See the legend in the next page)

Legend of Figure 3.6: A) Schematic representation of DCE-MRI experiment. After intraperitoneal injection of the contrast agent, 5 transgenic (Tg) and 7 wild type (WT) animals were subjected to MRI analysis using a 9.4 T magnetic resonance small animal scanner BioSpec 94/20. Adapted from (Maramraju, Junnarkar et al.) B) T1-weighted anatomical MRI image, showing the defined region of interest (ROI) in the cerebellum. C) Representative DCE-MRI images, acquired with a fat-saturated T1-weighted gradient-echo sequence, of a wild type and a transgenic mouse, respectively; signal intensity scale is given on the left side of the image. D) Tissue enhancement curve produced by the contrast agent in the plasma and in the tissue interstitium using DCE-MRI. MJD transgenic mice showed higher perfusion (i) and cerebellar blood volume (ii), as well as an increased capillary permeability (iii) and contrast agent accumulation in the cerebellum interstitium (iv), as compared to wild type controls. Each time unit in the graph corresponds to 125s, the scan time per dynamic. E) Quantification of total tissue enhancement produced by the circulation of contrast agent in the plasma and in the interstitium, here represented as the area under the curve (AUC) in arbitrary units (a.u.) showed a significant increase in MJD mice. Unpaired t-test, $p>0.05$= not significant and *$p\leq0.05$.

To investigate whether CNS-barriers disruption might be detected in live animals through a non-invasive method, two weeks before sacrifice, transgenic and age-matched wild type animals were analyzed by the DCE-MRI (see schematic presentation in Figure 3.6 A). A selected ROI was defined to the cerebellum (Figure 3.6 B) and the signal intensity resulting from contrast agent circulation in capillaries was recorded throughout time. As illustrated in Figure 3.6 C, the circulation of the contrast agent revealed a boost in signal intensity in the cerebellum of MJD mice, which was much lower in wild type animals. In agreement, the curve of variation of the signal intensity suggested higher blood volume in the cerebellum of transgenic mice, as the first signal intensity peak was higher (Figure 3.6 D – i and ii). In addition, the curve after the first peak, which represents the permeability-surface area product of the blood vessels, was also higher in MJD mice (Figure 3.6 D – iii). Consequently, the final part of the curve revealed the accumulation of the contrast agent in cerebellum interstitium of transgenic animals (Figure 3.6 D – iv).

Overall, MJD transgenic mice showed significant increased perfusion, vascular permeability and interstitial accumulation of contrast agent in the cerebellum as compared to wild type animals ($p=0.05$) (Figure 3.6 E). This result reveals that a higher amount of contrast agent has passed through blood capillaries and accumulated in the cerebellar interstitium of transgenic animals, in comparison to wild type animals. Apart from that, we showed that DCE-MRI allows an *in vivo* monitoring of CNS-barriers disruption in animal models by a non-invasive way.

4. Discussion

Central Nervous System (CNS) activity depends on a highly controlled environment, in part, provided by CNS-barriers, namely blood-brain barrier (BBB) and blood-cerebrospinal fluid barrier (BCSFB).

BBB is essential to brain homeostasis and CNS protection, since it controls the traffic of molecules, cells and other substances. In addition, it also provides the necessary nutrients to neuronal activity. Brain endothelial cells and pericytes wrapped in the basement membrane, as well as astrocytes are the main components responsible for the assembly of this barrier (Abbott et al 2010). Peculiar endothelial properties allow the reduced permeability of brain blood vessels. At the paracellular level, tight junctions (TJ) reduce the space between adjacent brain endothelial cells, restricting the solute movement between them, while the transcellular transport is reduced due to low and specific pinocytotic activity (Almutairi et al 2016).

BCSF is formed by epithelial cells in the choroid plexus and its function is to restrict the contact between blood and the (cerebrospinal fluid) CSF present in the ventricles These epithelial cells surround the choroid plexus parenchyma and capillaries, limiting the communication with CSF through TJ expression, the junctional complexes essential to restrict paracellular permeability (Engelhardt & Sorokin 2009).

Many neurodegenerative disorders involve CNS-barriers dysfunction at a certain level. The disarrangement of these structures usually leads to increased permeability of brain blood vessels and, consequently, the brain parenchyma becomes vulnerable to toxic blood-born substances, viruses, systemic inflammation and other threats to neuronal homeostasis. As reviewed by Zlokovic and colleagues, Alzheimer's, Parkinson's, Multiple Sclerosis, Huntington's and Amyotrophic Lateral Sclerosis, among other CNS diseases have been related to BBB disruption (Zlokovic 2008). In general, BBB dysfunction is associated with loss of TJs integrity, due to alterations in the expression of the associated proteins, lack of proper function, redistribution or degradation.

Despite the fact that BBB integrity and cerebrovascular network have been proven to be affected in neurodegenerative disorders, in Machado-Joseph Disease (MJD) this subject is poorly understood. Based on that, the main aim of the present study was to evaluate BBB integrity in this disease. MJD is a polyglutamine (polyQ) disorder and also the most common autosomal dominantly inherited spinocerebellar ataxia (SCA) worldwide. This neurodegenerative disease is caused by a CAG triplet expansion in the coding region of *MJD1/ATXN3* gene, which leads to a polyQ expansion in the respective protein ataxin-3. One of the hallmarks of this disease is the formation of mutant ataxin-3 aggregates, which are associated with several pathogenic mechanisms, such as dysfunction of quality-control mechanisms, mitochondrial abnormalities, transcriptional dysregulation and affected calcium homeostasis (Paulson et al 1997), as reviewed in (Nóbrega 2012 307).

In the present study we selected a transgenic mouse model of MJD previously developed by Torashima and collaborators. This model expresses a truncated form of human ataxin-3 with 69 CAG repeats under the control of L7 promoter, which results in the expression of this mutant protein specifically in Purkinje cells of the cerebellum (Torashima et al 2008). To investigate BBB integrity in this MJD model, transgenic and age-matched wild type littermates were firstly injected with Evans blue (EB) to evaluate BBB permeability. Next, in a second experiment, we assessed the mechanisms underlying BBB alterations, such as the presence of mutant ataxin-3 in cerebellar blood vessels, fibrin extravasation or TJ-associated protein alterations. Mice were also screened by (Dynamic Contrast-Enhanced-Magnetic Resonance Imaging) DCE-MRI, a non-invasive assay to evaluate cerebellar vascular changes.

EB has been widely used to study BBB permeability. Its injection in the caudal vein allows it to bind to albumin and reach brain capillaries; however, EB only enters into CNS parenchyma if BBB is disrupted (Rössner & Tempel 1966). In the cerebellum of the transgenic animal model

used in this study, EB dye extravasation was significantly increased as compared to wild type controls (Figure 3.1). However, no significant differences were found in the cerebrum of transgenic animals, which can be probably explained by the promoter used to drive the transgene expression in this specific mouse model - the L7 promoter. This promoter leads to the expression of mutant ataxin-3 only in Purkinje cells of the cerebellum, which means that alterations are mainly confined to this brain structure. Fluorescence microscopy confirmed the EB extravasation in the cerebellum of MJD transgenic mice and revealed that it was more abundant in DCN and lobules 8, 9 and 10 (Figure 3.1 F). Overall, the first experiment of this work provided clear evidences of BBB disruption in MJD.

After the EB evidences of BBB disruption in the cerebellum of MJD mice, it became relevant to investigate if mutant ataxin-3 was present in cerebellar blood vessels of the cerebellum. In fact, a double-immunofluorescence staining confirmed that mutant ataxin-3 aggregates were within cerebellar blood vessels (Figure 3.2). Since in this transgenic animal model mutant ataxin-3 expression is restricted to Purkinje cells, this provided evidence that this protein is possibly transmitted between cells. A similar observation was recently made for another polyQ disorder (Huntington's disease), in which it was suggested that the associated pathology is not strictly cell-autonomous and that huntingtin aggregates can spread between cells (Cicchetti et al 2014, Drouin-Ouellet et al 2015). In that way, it is plausible to think that mutant ataxin-3 aggregates accumulation within blood vessels could promote vascular alterations in the cerebellum of MJD transgenic mice.

In fact, (collagen IV) CoIV immunostaining suggested an increase in the density of cerebellar blood vessels in MJD mice when compared to wild type age-matched control subjects. Similar results were observed in patients and in a mouse model of Huntington's disease. The authors explained the increase in vessel density as an attempt to compensate the reduced oxygen delivery in the affected regions of the brain, by forming new blood vessels and promote oxygenation (Drouin-Ouellet et al 2015).

Next, to confirm whether the morphological changes seen in cerebellar blood vessels of MJD were associated with functional impairments of the BBB, the extravasation of fibrin through BBB was also assessed. Higher levels of extravascular fibrin were observed in transgenic mice, which confirmed BBB disruption (Figure 3.4 B). Altogether these results support the data from experiment 1, showing that BBB is compromised in MJD allowing blood-borne proteins, namely albumin and fibrin, to access the CNS.

After confirming extravasation of blood-borne proteins into the cerebellum of the MJD transgenic mice, it became relevant to assess the expression of TJ-associated proteins by Western blotting, as they are one of the key features of CNS-barriers.

One of the TJ-associated proteins is occludin, a transmembrane protein constituted by two domains: a long cytoplasmic C-terminal domain and the extracellular N-terminal (Li et al 2005). In the Western blot analysis, protein extracts from the cerebellum of MJD animals revealed an occludin band of lower molecular weight, corresponding to a 55kDa fragment, that was practically absent in wild type protein extracts (Figure 3.5 G). According to the literature, this fragment corresponds to the cytoplasmic C-terminal of occludin, lacking the transmembrane domain (Ghassemifar et al 2002, Li et al 2005). This suggests that occludin was cleaved in MJD mice. Similar evidence for occludin fragmentation in brain was already demonstrated in early ischemic stroke and bacterial meningitis, and was related to metalloproteinases (MMPs) activity. Specifically, MMP-2, 9 and 8 were identified as responsible for occludin cleavage (Liu et al 2012, Schubert-Unkmeir et al 2010). In fact, it is well known that: i) inflammatory response regulates MMPs expression and secretion (Yong 2005); ii) in MJD there is an increase in neuroinflammation, as seen by the increase in reactive astrocytes, activated microglial cells and pro-inflammatory cytokines interleukin-1 and 6 (Evert et al 2001). Moreover, it was also suggested that unlike wild type ataxin-3, the mutant form loses its ability to repress transcription of MMP-2 gene, leading to increased expression of this metalloproteinase (Evert et al 2001). Based on that, it is plausible to postulate that occludin degradation observed in this transgenic mouse model may

be explained by MMP2-mediated cleavage, a protein that is present in higher levels in the presence of mutant ataxin-3.

Claudin-5 is another transmembrane protein essential for the TJ assembly which is exclusively present in BBB. In several neurodegenerative disorders involving BBB dysfunction, such as Huntington's and Alzheimer's disease, this TJ-associated protein suffers alterations, frequently a decrease in its expression or redistribution (Drouin-Ouellet et al 2015, Marco & Skaper 2006). Surprisingly, in the cerebellum of MJD transgenic animals, Claudin-5 was significantly increased (Figure 3.5 H). In fact, some authors have already explained that in cases of BBB dysfunction this increment in claudin-5 expression may be a compensatory mechanism due to Occludin degradation, however, its redistribution from the membrane to the cytoplasm did not preserve BBB integrity (Fiorentino et al 2016, Liu et al 2012). In the case of Huntington's disease, for instance, recent studies performed in an *in vitro* BBB model (human brain microvascular endothelial cells derived from induced pluripotent stem cells) showed that claudin-5 is mainly found in the cytoplasm of brain endothelial cells and that indeed this redistribution is mainly related with increased levels of proteins associated with transcytosis (Drouin-Ouellet et al 2015, Lim et al 2017).

Zonula occludens 1 (ZO-1) expression levels were also analyzed. This cytoplasmic protein attach transmembrane proteins, such as Occludin and Claudin-5 to the actin cytoskeleton (Li et al 2005). There are two different ZO-1 isoforms: α+ is mainly found in epithelial cells, such as in choroid plexus TJs; the α- isoform, in the brain, is specific for the endothelium (Willott et al 1992).

In MJD transgenic mice, the levels ZO-1 α-, the one related to BBB, showed no significant differences compared to wild type animals (Figure 3.5 E). Nevertheless, there are other cell types expressing ZO-1, namely astrocytes and neurons (Miragall et al 1994). So, the relative expression levels of ZO-1 obtained in this study were not, exclusively, related to ZO-1 from TJs. Conversely, the isoform related with BCSFB (ZO-1 α+) demonstrated a strong tendency to decrease in MJD mice (Figure 3.5 C). This result suggests that BCSFB is compromised, since as a component of epithelial TJs, this protein is necessary to maintain low paracellular permeability.

These results suggest that ZO-1 protein expression in BBB is not affected in MJD mice, while in BCSFB the TJ assembly may be compromised, as ZO-1 isoform α+ is reduced in this mouse model. However, further studies need to be done to evaluate BCSFB activity in this MJD model.

In parallel, both transgenic and wild type mice were analyzed through DCE-MRI. MJD transgenic mice presented an increased blood volume, higher vascular permeability and consequent higher accumulation of the contrast agent in the cerebellum interstitium, as compared to age-matched controls (Figure 3.6 D). All of this confirmed and supported our previous evidences about BBB impairment, as well as BCSFB disruption in MJD.

Apart from that, we clearly demonstrated that DCE-MRI allows a non-invasive monitoring of CNS barriers in animal models.

Taken all of this into account, a mechanism for BBB disruption in MJD can be postulated, which is represented in Figure 4.1. In this way, one can hypothesize that ataxin-3 aggregation in neurovascular unit cells may produce BBB disarrangements leading to its dysfunction. In fact, as herein referred, ataxin-3 aggregates are known to activate neuroinflammation (Evert et al 2001). Because of that, there is a wide dysregulation in the levels of expression/activity of MMPs, a group of proteins essential for the endothelium modulation, as reviewed in (Rempe et al 2016). Furthermore, it has been demonstrated that mutant ataxin-3 directly upregulates MMP-2 expression (Evert et al 2006). In turn, MMPs, as modulators of the endothelium, affect TJs through degradation of its associated proteins. MMP-2, in particular, is known to mediate degradation of occludin which, in our work, was also demonstrated to occur in MJD transgenic mice. Since occludin was degraded, the transmembrane component of TJs becomes vulnerable (Liu et al 2012). This vulnerability can result in the attempt of the endothelium to compensate occludin degradation with the increased expression of claudin-5, another transmembrane protein

of endothelial TJs. However, it was recently demonstrated that the increased claudin-5 expression did not restore BBB integrity (Lim et al 2017). This is mainly due to its redistribution; claudin-5 is relocated from the membrane, where it exerts its function, to the cytoplasm. More important, this redistribution has been related to increased levels of vesicular transcellular transport (Drouin-Ouellet et al 2015). Based on that, and taking into account the results of albumin and fibrin extravasation, it is expected that transcytosis is also increased in the BBB of MJD transgenic mice, since these macromolecules usually overcome the endothelial barrier by transcellular transport (Lim et al 2017).

On the other hand, in the BCSFB, the TJs' assembly may be also compromised due to occludin degradation and the tendency to show reduced expression of the α+ isoform of ZO-1. Both proteins may also be affected by increased inflammation and consequent MMPs dysregulation.

Since CNS-barriers' role is essential to maintain brain homeostasis, BBB and BCSFB disruption could also contribute to MJD-associated neuropathology and enhance its inherent neuroinflammation. On the opposite side, in a pharmacological perspective of view, despite the negative effect of an increased CNS-barriers permeability, it can be seen as an opportunity to use many therapeutic agents that until now were thought to be incapable to cross these barriers, to actually reach the CNS.

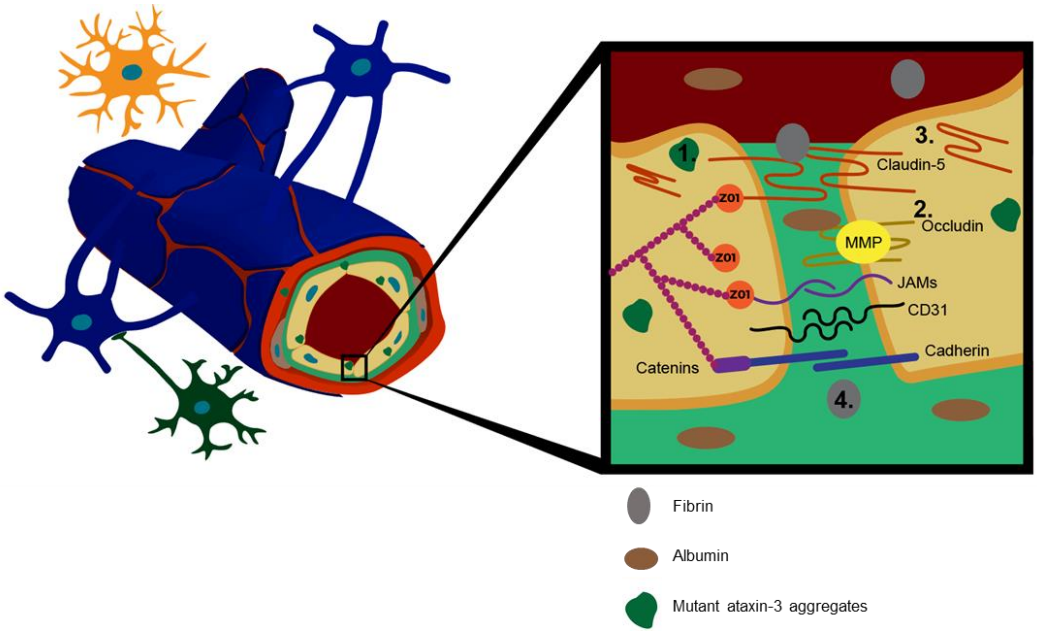

Figure 4.1. Schematic representation of the neurovascular unit impairments in MJD according to the theory postulated in the present study. The presence of mutant ataxin-3 aggregates in the BBB of the MJD mouse model (1) may upregulate MMPs activity, which mediate Occludin degradation (2). Consequently, there is an attempt to compensate this occludin degradation through an increment in claudin-5 expression (3), which is not sufficient to restore BBB properties. Thus, BBB became dysfunctional leading to extravasation of blood-born proteins (4).

5. References

Abbott NJ, Patabendige AA, Dolman DE, Yusof SR, Begley DJ. 2010. Structure and function of the blood-brain barrier. *Neurobiol Dis* 37: 13-25

Abbott NJ, Ronnback L, Hansson E. 2006. Astrocyte-endothelial interactions at the blood-brain barrier. *Nat Rev Neurosci* 7: 41-53

Aliev G, Palacios HH, Lipsitt AE, Fischbach K, Lamb BT, et al. 2009. Nitric oxide as an initiator of brain lesions during the development of Alzheimer disease. *Neurotox Res* 16: 293-305

Allinson KR, Lee HS, Fruttiger M, McCarty JH, Arthur HM. 2012. Endothelial expression of TGFbeta type II receptor is required to maintain vascular integrity during postnatal development of the central nervous system. *PLoS One* 7: e39336

Almutairi MM, Gong C, Xu YG, Chang Y, Shi H. 2016. Factors controlling permeability of the blood-brain barrier. *Cellular and molecular life sciences : CMLS* 73: 57-77

Anderson CM, Nedergaard M. 2003. Astrocyte-mediated control of cerebral microcirculation. *Trends Neurosci* 26: 340-4; author reply 44-5

Armulik A, Genove G, Mae M, Nisancioglu MH, Wallgard E, et al. 2010. Pericytes regulate the blood-brain barrier. *Nature* 468: 557-61

Arnold T, Betsholtz C. 2013. The importance of microglia in the development of the vasculature in the central nervous system. *Vascular cell* 5: 4

Ashkenazi A, Bento CF, Ricketts T, Vicinanza M, Siddiqi F, et al. 2017. Polyglutamine tracts regulate beclin 1-dependent autophagy. *Nature* 545: 108-11

Banks WA. 2016. From blood-brain barrier to blood-brain interface: new opportunities for CNS drug delivery. *Nature reviews. Drug discovery* 15: 275-92

Bartels AL. 2011. Blood-brain barrier P-glycoprotein function in neurodegenerative disease. *Curr Pharm Des* 17: 2771-7

Bauer HC, Krizbai IA, Bauer H, Traweger A. 2014. "You Shall Not Pass"-tight junctions of the blood brain barrier. *Frontiers in neuroscience* 8: 392

Bazzoni G, Dejana E. 2004. Endothelial cell-to-cell junctions: molecular organization and role in vascular homeostasis. *Physiol Rev* 84: 869-901

Bazzoni G, Martinez-Estrada OM, Mueller F, Nelboeck P, Schmid G, et al. 2000a. Homophilic interaction of junctional adhesion molecule. *J Biol Chem* 275: 30970-6

Bazzoni G, Martinez-Estrada OM, Orsenigo F, Cordenonsi M, Citi S, Dejana E. 2000b. Interaction of junctional adhesion molecule with the tight junction components ZO-1, cingulin, and occludin. *J Biol Chem* 275: 20520-6

Beaulieu E, Demeule M, Ghitescu L, Beliveau R. 1997. P-glycoprotein is strongly expressed in the luminal membranes of the endothelium of blood vessels in the brain. *The Biochemical journal* 326 (Pt 2): 539-44

Bechmann I, Kwidzinski E, Kovac AD, Simburger E, Horvath T, et al. 2001. Turnover of rat brain perivascular cells. *Experimental neurology* 168: 242-9

Begley DJ. 2004. ABC transporters and the blood-brain barrier. *Curr Pharm Des* 10: 1295-312

Bell RD, Sagare AP, Friedman AE, Bedi GS, Holtzman DM, et al. 2007. Transport pathways for clearance of human Alzheimer's amyloid beta-peptide and apolipoproteins E and J in the mouse central nervous system. *J Cereb Blood Flow Metab* 27: 909-18

Berke SJ, Chai Y, Marrs GL, Wen H, Paulson HL. 2005. Defining the role of ubiquitin-interacting motifs in the polyglutamine disease protein, ataxin-3. *J Biol Chem* 280: 32026-34

Berke SJ, Schmied FA, Brunt ER, Ellerby LM, Paulson HL. 2004. Caspase-mediated proteolysis of the polyglutamine disease protein ataxin-3. *J Neurochem* 89: 908-18

Bernacki J, Dobrowolska A, Nierwinska K, Malecki A. 2008. Physiology and pharmacological role of the blood-brain barrier. *Pharmacol Rep* 60: 600-22

Betanzos A, Huerta M, Lopez-Bayghen E, Azuara E, Amerena J, Gonzalez-Mariscal L. 2004. The tight junction protein ZO-2 associates with Jun, Fos and C/EBP transcription factors in epithelial cells. *Exp Cell Res* 292: 51-66

Bettencourt C, Lima M. 2011. Machado-Joseph Disease: from first descriptions to new perspectives. *Orphanet J Rare Dis* 6: 35

Bettencourt C, Santos C, Montiel R, Costa Mdo C, Cruz-Morales P, et al. 2010. Increased transcript diversity: novel splicing variants of Machado-Joseph disease gene (ATXN3). *Neurogenetics* 11: 193-202

Biernacki K, Prat A, Blain M, Antel JP. 2004. Regulation of cellular and molecular trafficking across human brain endothelial cells by Th1- and Th2-polarized lymphocytes. *J Neuropathol Exp Neurol* 63: 223-32

Blum-Degen D, Muller T, Kuhn W, Gerlach M, Przuntek H, Riederer P. 1995. Interleukin-1 beta and interleukin-6 are elevated in the cerebrospinal fluid of Alzheimer's and de novo Parkinson's disease patients. *Neuroscience letters* 202: 17-20

Bonkowski D, Katyshev V, Balabanov RD, Borisov A, Dore-Duffy P. 2011. The CNS microvascular pericyte: pericyte-astrocyte crosstalk in the regulation of tissue survival. *Fluids Barriers CNS* 8: 8

Boy J, Schmidt T, Schumann U, Grasshoff U, Unser S, et al. 2010. A transgenic mouse model of spinocerebellar ataxia type 3 resembling late disease onset and gender-specific instability of CAG repeats. *Neurobiol Dis* 37: 284-93

Bradford J, Shin JY, Roberts M, Wang CE, Li XJ, Li S. 2009. Expression of mutant huntingtin in mouse brain astrocytes causes age-dependent neurological symptoms. *Proc Natl Acad Sci U S A* 106: 22480-5

Brown GC, Neher JJ. 2014. Microglial phagocytosis of live neurons. *Nat Rev Neurosci* 15: 209-16

Browne SE, Ferrante RJ, Beal MF. 1999. Oxidative stress in Huntington's disease. *Brain Pathol* 9: 147-63

Bruck W, Bitsch A, Kolenda H, Bruck Y, Stiefel M, Lassmann H. 1997. Inflammatory central nervous system demyelination: correlation of magnetic resonance imaging findings with lesion pathology. *Ann Neurol* 42: 783-93

Burnett BG, Pittman RN. 2005. The polyglutamine neurodegenerative protein ataxin 3 regulates aggresome formation. *Proc Natl Acad Sci U S A* 102: 4330-5

Cabezas R, Avila M, Gonzalez J, El-Bacha RS, Baez E, et al. 2014. Astrocytic modulation of blood brain barrier: perspectives on Parkinson's disease. *Front Cell Neurosci* 8: 211

Caldeira C, Cunha C, Vaz AR, Falcao AS, Barateiro A, et al. 2017. Key Aging-Associated Alterations in Primary Microglia Response to Beta-Amyloid Stimulation. *Frontiers in aging neuroscience* 9: 277

Cardoso FL, Brites D, Brito MA. 2010. Looking at the blood-brain barrier: molecular anatomy and possible investigation approaches. *Brain research reviews* 64: 328-63

Cardoso FL, Herz J, Fernandes A, Rocha J, Sepodes B, et al. 2015. Systemic inflammation in early neonatal mice induces transient and lasting neurodegenerative effects. *J Neuroinflammation* 12: 82

Carmona V, Cunha-Santos J, Onofre I, Simoes AT, Vijayakumar U, et al. 2017. Unravelling Endogenous MicroRNA System Dysfunction as a New Pathophysiological Mechanism in Machado-Joseph Disease. *Molecular therapy : the journal of the American Society of Gene Therapy* 25: 1038-55

Carreno-Muller E, Herrera AJ, de Pablos RM, Tomas-Camardiel M, Venero JL, et al. 2003. Thrombin induces in vivo degeneration of nigral dopaminergic neurones along with the activation of microglia. *J Neurochem* 84: 1201-14

Carvalho DR, La Rocque-Ferreira A, Rizzo IM, Imamura EU, Speck-Martins CE. 2008. Homozygosity enhances severity in spinocerebellar ataxia type 3. *Pediatr Neurol* 38: 296-9

Cemal CK, Carroll CJ, Lawrence L, Lowrie MB, Ruddle P, et al. 2002. YAC transgenic mice carrying pathological alleles of the MJD1 locus exhibit a mild and slowly progressive cerebellar deficit. *Hum Mol Genet* 11: 1075-94

Chai Y, Koppenhafer SL, Shoesmith SJ, Perez MK, Paulson HL. 1999. Evidence for proteasome involvement in polyglutamine disease: localization to nuclear inclusions in SCA3/MJD and suppression of polyglutamine aggregation in vitro. *Hum Mol Genet* 8: 673-82

Chang CY, Li JR, Chen WY, Ou YC, Lai CY, et al. 2015. Disruption of in vitro endothelial barrier integrity by Japanese encephalitis virus-Infected astrocytes. *Glia*

Chen X, Lan X, Roche I, Liu R, Geiger JD. 2008. Caffeine protects against MPTP-induced blood-brain barrier dysfunction in mouse striatum. *J Neurochem* 107: 1147-57

Chou AH, Yeh TH, Ouyang P, Chen YL, Chen SY, Wang HL. 2008. Polyglutamine-expanded ataxin-3 causes cerebellar dysfunction of SCA3 transgenic mice by inducing transcriptional dysregulation. *Neurobiol Dis* 31: 89-101

Cicchetti F, Lacroix S, Cisbani G, Vallieres N, Saint-Pierre M, et al. 2014. Mutant huntingtin is present in neuronal grafts in Huntington disease patients. *Ann Neurol* 76: 31-42

Claudio L, Raine CS, Brosnan CF. 1995. Evidence of persistent blood-brain barrier abnormalities in chronic-progressive multiple sclerosis. *Acta Neuropathol* 90: 228-38

Cordenonsi M, D'Atri F, Hammar E, Parry DA, Kendrick-Jones J, et al. 1999. Cingulin contains globular and coiled-coil domains and interacts with ZO-1, ZO-2, ZO-3, and myosin. *J Cell Biol* 147: 1569-82

Costa Mdo C, Paulson HL. 2012. Toward understanding Machado-Joseph disease. *Prog Neurobiol* 97: 239-57

Cuenod CA, Balvay D. 2013. Perfusion and vascular permeability: basic concepts and measurement in DCE-CT and DCE-MRI. *Diagnostic and interventional imaging* 94: 1187-204

Cuevas P, Gutierrez-Diaz JA, Reimers D, Dujovny M, Diaz FG, Ausman JI. 1984. Pericyte endothelial gap junctions in human cerebral capillaries. *Anat Embryol (Berl)* 170: 155-9

Daneman R, Zhou L, Kebede AA, Barres BA. 2010. Pericytes are required for blood-brain barrier integrity during embryogenesis. *Nature* 468: 562-6

Darland DC, Massingham LJ, Smith SR, Piek E, Saint-Geniez M, D'Amore PA. 2003. Pericyte production of cell-associated VEGF is differentiation-dependent and is associated with endothelial survival. *Developmental biology* 264: 275-88

Davoust N, Vuaillat C, Androdias G, Nataf S. 2008. From bone marrow to microglia: barriers and avenues. *Trends Immunol* 29: 227-34

Deane R, Wu Z, Zlokovic BV. 2004. RAGE (yin) versus LRP (yang) balance regulates alzheimer amyloid beta-peptide clearance through transport across the blood-brain barrier. *Stroke* 35: 2628-31

Deo AK, Borson S, Link JM, Domino K, Eary JF, et al. 2014. Activity of P-Glycoprotein, a beta-Amyloid Transporter at the Blood-Brain Barrier, Is Compromised in Patients with Mild Alzheimer Disease. *Journal of nuclear medicine : official publication, Society of Nuclear Medicine* 55: 1106-11

do Carmo Costa M, Bajanca F, Rodrigues AJ, Tome RJ, Corthals G, et al. 2010. Ataxin-3 plays a role in mouse myogenic differentiation through regulation of integrin subunit levels. *PLoS One* 5: e11728

Dohgu S, Yamauchi A, Takata F, Naito M, Tsuruo T, et al. 2004. Transforming growth factor-beta1 upregulates the tight junction and P-glycoprotein of brain microvascular endothelial cells. *Cell Mol Neurobiol* 24: 491-7

Drouin-Ouellet J, Sawiak SJ, Cisbani G, Lagace M, Kuan WL, et al. 2015. Cerebrovascular and blood-brain barrier impairments in Huntington's disease: Potential implications for its pathophysiology. *Ann Neurol* 78: 160-77

Dudvarski Stankovic N, Teodorczyk M, Ploen R, Zipp F, Schmidt MH. 2016. Microglia-blood vessel interactions: a double-edged sword in brain pathologies. *Acta Neuropathol* 131: 347-63

Eisele P, Alonso A, Griebe M, Szabo K, Hennerici MG, Gass A. 2016. Investigation of cerebral microbleeds in multiple sclerosis as a potential marker of blood-brain barrier dysfunction. *Multiple sclerosis and related disorders* 7: 61-4

Elahy M, Jackaman C, Mamo JC, Lam V, Dhaliwal SS, et al. 2015. Blood-brain barrier dysfunction developed during normal aging is associated with inflammation and loss of tight junctions but not with leukocyte recruitment. *Immunity & ageing : I & A* 12: 2

Ellisdon AM, Thomas B, Bottomley SP. 2006. The two-stage pathway of ataxin-3 fibrillogenesis involves a polyglutamine-independent step. *J Biol Chem* 281: 16888-96

Engelhardt B, Sorokin L. 2009. The blood-brain and the blood-cerebrospinal fluid barriers: function and dysfunction. *Seminars in immunopathology* 31: 497-511

Evers MM, Toonen LJ, van Roon-Mom WM. 2014. Ataxin-3 protein and RNA toxicity in spinocerebellar ataxia type 3: current insights and emerging therapeutic strategies. *Mol Neurobiol* 49: 1513-31

Evert BO, Araujo J, Vieira-Saecker AM, de Vos RA, Harendza S, et al. 2006. Ataxin-3 represses transcription via chromatin binding, interaction with histone deacetylase 3, and histone deacetylation. *J Neurosci* 26: 11474-86

Evert BO, Vogt IR, Kindermann C, Ozimek L, de Vos RA, et al. 2001. Inflammatory genes are upregulated in expanded ataxin-3-expressing cell lines and spinocerebellar ataxia type 3 brains. *J Neurosci* 21: 5389-96

Evert BO, Vogt IR, Vieira-Saecker AM, Ozimek L, de Vos RA, et al. 2003. Gene expression profiling in ataxin-3 expressing cell lines reveals distinct effects of normal and mutant ataxin-3. *J Neuropathol Exp Neurol* 62: 1006-18

Farkas E, De Jong GI, Apro E, De Vos RA, Steur EN, Luiten PG. 2000. Similar ultrastructural breakdown of cerebrocortical capillaries in Alzheimer's disease, Parkinson's disease, and experimental hypertension. What is the functional link? *Ann N Y Acad Sci* 903: 72-82

Feletou M. 2011. In *The Endothelium: Part 1: Multiple Functions of the Endothelial Cells-Focus on Endothelium-Derived Vasoactive Mediators*. San Rafael (CA)

Filous AR, Silver J. 2016. "Targeting astrocytes in CNS injury and disease: A translational research approach". *Prog Neurobiol*

Findley MK, Koval M. 2009. Regulation and roles for claudin-family tight junction proteins. *IUBMB life* 61: 431-7

Fiorentino M, Sapone A, Senger S, Camhi SS, Kadzielski SM, et al. 2016. Blood-brain barrier and intestinal epithelial barrier alterations in autism spectrum disorders. *Molecular autism* 7: 49

Franciosi S, Ryu JK, Shim Y, Hill A, Connolly C, et al. 2012. Age-dependent neurovascular abnormalities and altered microglial morphology in the YAC128 mouse model of Huntington disease. *Neurobiol Dis* 45: 438-49

Franklin KBJ, Paxinos G. 2001. The mouse brain in stereotaxic coordinates. [San Diego u.a.: Acad. Press

Gatchel JR, Zoghbi HY. 2005. Diseases of unstable repeat expansion: mechanisms and common principles. *Nature reviews. Genetics* 6: 743-55

Ghassemifar MR, Sheth B, Papenbrock T, Leese HJ, Houghton FD, Fleming TP. 2002. Occludin TM4(-): an isoform of the tight junction protein present in primates lacking the fourth transmembrane domain. *J Cell Sci* 115: 3171-80

Gingrich MB, Traynelis SF. 2000. Serine proteases and brain damage - is there a link? *Trends Neurosci* 23: 399-407

Gonzalez-Scarano F, Baltuch G. 1999. Microglia as mediators of inflammatory and degenerative diseases. *Annual review of neuroscience* 22: 219-40

Gray MT, Woulfe JM. 2015. Striatal blood-brain barrier permeability in Parkinson's disease. *J Cereb Blood Flow Metab* 35: 747-50

Gu XL, Long CX, Sun L, Xie C, Lin X, Cai H. 2010. Astrocytic expression of Parkinson's disease-related A53T alpha-synuclein causes neurodegeneration in mice. *Mol Brain* 3: 12

Guerriero F, Sgarlata C, Francis M, Maurizi N, Faragli A, et al. 2016. Neuroinflammation, immune system and Alzheimer disease: searching for the missing link. *Aging clinical and experimental research*

Gunzel D, Yu AS. 2013. Claudins and the modulation of tight junction permeability. *Physiol Rev* 93: 525-69

Halliday MR, Rege SV, Ma Q, Zhao Z, Miller CA, et al. 2016. Accelerated pericyte degeneration and blood-brain barrier breakdown in apolipoprotein E4 carriers with Alzheimer's disease. *J Cereb Blood Flow Metab* 36: 216-27

Hamilton NB, Attwell D, Hall CN. 2010. Pericyte-mediated regulation of capillary diameter: a component of neurovascular coupling in health and disease. *Frontiers in neuroenergetics* 2

Haorah J, Heilman D, Knipe B, Chrastil J, Leibhart J, et al. 2005. Ethanol-induced activation of myosin light chain kinase leads to dysfunction of tight junctions and blood-brain barrier compromise. *Alcoholism, clinical and experimental research* 29: 999-1009

Haseloff RF, Blasig IE, Bauer HC, Bauer H. 2005. In search of the astrocytic factor(s) modulating blood-brain barrier functions in brain capillary endothelial cells in vitro. *Cell Mol Neurobiol* 25: 25-39

Hawkins BT, Davis TP. 2005. The blood-brain barrier/neurovascular unit in health and disease. *Pharmacological reviews* 57: 173-85

Hirase T, Kawashima S, Wong EY, Ueyama T, Rikitake Y, et al. 2001. Regulation of tight junction permeability and occludin phosphorylation by Rhoa-p160ROCK-dependent and -independent mechanisms. *J Biol Chem* 276: 10423-31

Hirase T, Staddon JM, Saitou M, Ando-Akatsuka Y, Itoh M, et al. 1997. Occludin as a possible determinant of tight junction permeability in endothelial cells. *J Cell Sci* 110 (Pt 14): 1603-13

Hsiao HY, Chen YC, Huang CH, Chen CC, Hsu YH, et al. 2015. Aberrant astrocytes impair vascular reactivity in Huntington disease. *Ann Neurol* 78: 178-92

Huber JD, Egleton RD, Davis TP. 2001. Molecular physiology and pathophysiology of tight junctions in the blood-brain barrier. *Trends Neurosci* 24: 719-25

Ichikawa Y, Goto J, Hattori M, Toyoda A, Ishii K, et al. 2001. The genomic structure and expression of MJD, the Machado-Joseph disease gene. *J Hum Genet* 46: 413-22

Igarashi S, Takiyama Y, Cancel G, Rogaeva EA, Sasaki H, et al. 1996. Intergenerational instability of the CAG repeat of the gene for Machado-Joseph disease (MJD1) is affected by the genotype of the normal chromosome: implications for the molecular mechanisms of the instability of the CAG repeat. *Hum Mol Genet* 5: 923-32

Igarashi Y, Utsumi H, Chiba H, Yamada-Sasamori Y, Tobioka H, et al. 1999. Glial cell line-derived neurotrophic factor induces barrier function of endothelial cells forming the blood-brain barrier. *Biochemical and biophysical research communications* 261: 108-12

Ikeda H, Yamaguchi M, Sugai S, Aze Y, Narumiya S, Kakizuka A. 1996. Expanded polyglutamine in the Machado-Joseph disease protein induces cell death in vitro and in vivo. *Nat Genet* 13: 196-202

Jaeger LB, Dohgu S, Hwang MC, Farr SA, Murphy MP, et al. 2009. Testing the neurovascular hypothesis of Alzheimer's disease: LRP-1 antisense reduces blood-brain barrier clearance, increases brain levels of amyloid-beta protein, and impairs cognition. *J Alzheimers Dis* 17: 553-70

Janzer RC, Raff MC. 1987. Astrocytes induce blood-brain barrier properties in endothelial cells. *Nature* 325: 253-7

Jardim LB, Pereira ML, Silveira I, Ferro A, Sequeiros J, Giugliani R. 2001. Neurologic findings in Machado-Joseph disease: relation with disease duration, subtypes, and (CAG)n. *Arch Neurol* 58: 899-904

Jeansson M, Gawlik A, Anderson G, Li C, Kerjaschki D, et al. 2011. Angiopoietin-1 is essential in mouse vasculature during development and in response to injury. *J Clin Invest* 121: 2278-89

Jolivel V, Bicker F, Biname F, Ploen R, Keller S, et al. 2015. Perivascular microglia promote blood vessel disintegration in the ischemic penumbra. *Acta Neuropathol* 129: 279-95

Jones AR, Shusta EV. 2007. Blood-brain barrier transport of therapeutics via receptor-mediation. *Pharmaceutical research* 24: 1759-71

Kale G, Naren AP, Sheth P, Rao RK. 2003. Tyrosine phosphorylation of occludin attenuates its interactions with ZO-1, ZO-2, and ZO-3. *Biochemical and biophysical research communications* 302: 324-9

Katsuno T, Umeda K, Matsui T, Hata M, Tamura A, et al. 2008. Deficiency of zonula occludens-1 causes embryonic lethal phenotype associated with defected yolk sac angiogenesis and apoptosis of embryonic cells. *Mol Biol Cell* 19: 2465-75

Kawaguchi Y, Okamoto T, Taniwaki M, Aizawa M, Inoue M, et al. 1994. CAG expansions in a novel gene for Machado-Joseph disease at chromosome 14q32.1. *Nat Genet* 8: 221-8

Kazachkova N, Raposo M, Montiel R, Cymbron T, Bettencourt C, et al. 2013. Patterns of mitochondrial DNA damage in blood and brain tissues of a transgenic mouse model of Machado-Joseph disease. *Neuro-degenerative diseases* 11: 206-14

Kolarova H, Ambruzova B, Svihalkova Sindlerova L, Klinke A, Kubala L. 2014. Modulation of endothelial glycocalyx structure under inflammatory conditions. *Mediators of inflammation* 2014: 694312

Kooij G, Kopplin K, Blasig R, Stuiver M, Koning N, et al. 2014. Disturbed function of the blood-cerebrospinal fluid barrier aggravates neuro-inflammation. *Acta Neuropathol* 128: 267-77

Kooij G, van Horssen J, de Lange EC, Reijerkerk A, van der Pol SM, et al. 2010. T lymphocytes impair P-glycoprotein function during neuroinflammation. *Journal of autoimmunity* 34: 416-25

Kook SY, Seok Hong H, Moon M, Mook-Jung I. 2013. Disruption of blood-brain barrier in Alzheimer disease pathogenesis. *Tissue barriers* 1: e23993

Kortekaas R, Leenders KL, van Oostrom JC, Vaalburg W, Bart J, et al. 2005. Blood-brain barrier dysfunction in parkinsonian midbrain in vivo. *Ann Neurol* 57: 176-9

Laco MN, Cortes L, Travis SM, Paulson HL, Rego AC. 2012a. Valosin-containing protein (VCP/p97) is an activator of wild-type ataxin-3. *PLoS One* 7: e43563

Laco MN, Oliveira CR, Paulson HL, Rego AC. 2012b. Compromised mitochondrial complex II in models of Machado-Joseph disease. *Biochimica et biophysica acta* 1822: 139-49

Lam FC, Liu R, Lu P, Shapiro AB, Renoir JM, et al. 2001. beta-Amyloid efflux mediated by p-glycoprotein. *J Neurochem* 76: 1121-8

Larochelle C, Alvarez JI, Prat A. 2011. How do immune cells overcome the blood-brain barrier in multiple sclerosis? *FEBS Lett* 585: 3770-80

Lassmann H, Bruck W, Lucchinetti CF. 2007. The immunopathology of multiple sclerosis: an overview. *Brain Pathol* 17: 210-8
Lecuyer MA, Kebir H, Prat A. 2016. Glial influences on BBB functions and molecular players in immune cell trafficking. *Biochimica et biophysica acta* 1862: 472-82
Lee G, Bendayan R. 2004. Functional expression and localization of P-glycoprotein in the central nervous system: relevance to the pathogenesis and treatment of neurological disorders. *Pharmaceutical research* 21: 1313-30
Lee JY, Kim HS, Choi HY, Oh TH, Yune TY. 2012. Fluoxetine inhibits matrix metalloprotease activation and prevents disruption of blood-spinal cord barrier after spinal cord injury. *Brain* 135: 2375-89
LeVine SM. 2016. Albumin and multiple sclerosis. *BMC neurology* 16: 47
Li F, Lan Y, Wang Y, Wang J, Yang G, et al. 2011. Endothelial Smad4 maintains cerebrovascular integrity by activating N-cadherin through cooperation with Notch. *Developmental cell* 20: 291-302
Li F, Macfarlan T, Pittman RN, Chakravarti D. 2002. Ataxin-3 is a histone-binding protein with two independent transcriptional corepressor activities. *J Biol Chem* 277: 45004-12
Li LB, Yu Z, Teng X, Bonini NM. 2008. RNA toxicity is a component of ataxin-3 degeneration in Drosophila. *Nature* 453: 1107-11
Li Y, Fanning AS, Anderson JM, Lavie A. 2005. Structure of the conserved cytoplasmic C-terminal domain of occludin: identification of the ZO-1 binding surface. *Journal of molecular biology* 352: 151-64
Liddelow SA, Dziegielewska KM, Ek CJ, Habgood MD, Bauer H, et al. 2013. Mechanisms that determine the internal environment of the developing brain: a transcriptomic, functional and ultrastructural approach. *PLoS One* 8: e65629
Lim J, Crespo-Barreto J, Jafar-Nejad P, Bowman AB, Richman R, et al. 2008. Opposing effects of polyglutamine expansion on native protein complexes contribute to SCA1. *Nature* 452: 713-8
Lim RG, Quan C, Reyes-Ortiz AM, Lutz SE, Kedaigle AJ, et al. 2017. Huntington's Disease iPSC-Derived Brain Microvascular Endothelial Cells Reveal WNT-Mediated Angiogenic and Blood-Brain Barrier Deficits. *Cell reports* 19: 1365-77
Lima M, Costa MC, Montiel R, Ferro A, Santos C, et al. 2005. Population genetics of wild-type CAG repeats in the Machado-Joseph disease gene in Portugal. *Hum Hered* 60: 156-63
Liu J, Jin X, Liu KJ, Liu W. 2012. Matrix metalloproteinase-2-mediated occludin degradation and caveolin-1-mediated claudin-5 redistribution contribute to blood-brain barrier damage in early ischemic stroke stage. *J Neurosci* 32: 3044-57
Liu X, Tu M, Kelly RS, Chen C, Smith BJ. 2004. Development of a computational approach to predict blood-brain barrier permeability. *Drug Metab Dispos* 32: 132-9
Lopes Pinheiro MA, Kooij G, Mizee MR, Kamermans A, Enzmann G, et al. 2016. Immune cell trafficking across the barriers of the central nervous system in multiple sclerosis and stroke. *Biochimica et biophysica acta* 1862: 461-71
Loscher W, Potschka H. 2005. Blood-brain barrier active efflux transporters: ATP-binding cassette gene family. *NeuroRx* 2: 86-98
Maciel P, Lopes-Cendes I, Kish S, Sequeiros J, Rouleau GA. 1997. Mosaicism of the CAG repeat in CNS tissue in relation to age at death in spinocerebellar ataxia type 1 and Machado-Joseph disease patients. *Am J Hum Genet* 60: 993-6
Mackic JB, Bading J, Ghiso J, Walker L, Wisniewski T, et al. 2002. Circulating amyloid-beta peptide crosses the blood-brain barrier in aged monkeys and contributes to Alzheimer's disease lesions. *Vascul Pharmacol* 38: 303-13
Makarewicz D, Zieminska E, Lazarewicz JW. 2003. Dantrolene inhibits NMDA-induced 45Ca uptake in cultured cerebellar granule neurons. *Neurochemistry international* 43: 273-8
Mao Y, Senic-Matuglia F, Di Fiore PP, Polo S, Hodsdon ME, De Camilli P. 2005. Deubiquitinating function of ataxin-3: insights from the solution structure of the Josephin domain. *Proc Natl Acad Sci U S A* 102: 12700-5
Marco S, Skaper SD. 2006. Amyloid beta-peptide1-42 alters tight junction protein distribution and expression in brain microvessel endothelial cells. *Neuroscience letters* 401: 219-24
Martin-Padura I, Lostaglio S, Schneemann M, Williams L, Romano M, et al. 1998. Junctional adhesion molecule, a novel member of the immunoglobulin superfamily that distributes at intercellular junctions and modulates monocyte transmigration. *J Cell Biol* 142: 117-27

Masino L, Musi V, Menon RP, Fusi P, Kelly G, et al. 2003. Domain architecture of the polyglutamine protein ataxin-3: a globular domain followed by a flexible tail. *FEBS Lett* 549: 21-5
Matos CA, de Macedo-Ribeiro S, Carvalho AL. 2011. Polyglutamine diseases: the special case of ataxin-3 and Machado-Joseph disease. *Prog Neurobiol* 95: 26-48
Matsumura T, Wolff K, Petzelbauer P. 1997. Endothelial cell tube formation depends on cadherin 5 and CD31 interactions with filamentous actin. *J Immunol* 158: 3408-16
Matter K, Balda MS. 2003. Signalling to and from tight junctions. *Nat Rev Mol Cell Biol* 4: 225-36
Mazzucchelli S, De Palma A, Riva M, D'Urzo A, Pozzi C, et al. 2009. Proteomic and biochemical analyses unveil tight interaction of ataxin-3 with tubulin. *The international journal of biochemistry & cell biology* 41: 2485-92
Mealey KL, Greene S, Bagley R, Gay J, Tucker R, et al. 2008. P-glycoprotein contributes to the blood-brain, but not blood-cerebrospinal fluid, barrier in a spontaneous canine p-glycoprotein knockout model. *Drug Metab Dispos* 36: 1073-9
Michele DE, Campbell KP. 2003. Dystrophin-glycoprotein complex: post-translational processing and dystroglycan function. *J Biol Chem* 278: 15457-60
Miragall F, Krause D, de Vries U, Dermietzel R. 1994. Expression of the tight junction protein ZO-1 in the olfactory system: presence of ZO-1 on olfactory sensory neurons and glial cells. *The Journal of comparative neurology* 341: 433-48
Mizee MR, Nijland PG, van der Pol SM, Drexhage JA, van Het Hof B, et al. 2014. Astrocyte-derived retinoic acid: a novel regulator of blood-brain barrier function in multiple sclerosis. *Acta Neuropathol* 128: 691-703
Morgan L, Shah B, Rivers LE, Barden L, Groom AJ, et al. 2007. Inflammation and dephosphorylation of the tight junction protein occludin in an experimental model of multiple sclerosis. *Neuroscience* 147: 664-73
Morita K, Sasaki H, Furuse M, Tsukita S. 1999. Endothelial claudin: claudin-5/TMVCF constitutes tight junction strands in endothelial cells. *J Cell Biol* 147: 185-94
Morris AW, Carare RO, Schreiber S, Hawkes CA. 2014. The Cerebrovascular Basement Membrane: Role in the Clearance of beta-amyloid and Cerebral Amyloid Angiopathy. *Frontiers in aging neuroscience* 6: 251
Nadal A, Fuentes E, Pastor J, McNaughton PA. 1995. Plasma albumin is a potent trigger of calcium signals and DNA synthesis in astrocytes. *Proc Natl Acad Sci U S A* 92: 1426-30
Nagai Y, Inui T, Popiel HA, Fujikake N, Hasegawa K, et al. 2007. A toxic monomeric conformer of the polyglutamine protein. *Nat Struct Mol Biol* 14: 332-40
Nagasawa K, Chiba H, Fujita H, Kojima T, Saito T, et al. 2006. Possible involvement of gap junctions in the barrier function of tight junctions of brain and lung endothelial cells. *J Cell Physiol* 208: 123-32
Nascimento-Ferreira I, Santos-Ferreira T, Sousa-Ferreira L, Auregan G, Onofre I, et al. 2011. Overexpression of the autophagic beclin-1 protein clears mutant ataxin-3 and alleviates Machado-Joseph disease. *Brain* 134: 1400-15
Natalello A, Frana AM, Relini A, Apicella A, Invernizzi G, et al. 2011. A major role for side-chain polyglutamine hydrogen bonding in irreversible ataxin-3 aggregation. *PLoS One* 6: e18789
Newman EA. 2003. New roles for astrocytes: regulation of synaptic transmission. *Trends Neurosci* 26: 536-42
Nieset JE, Redfield AR, Jin F, Knudsen KA, Johnson KR, Wheelock MJ. 1997. Characterization of the interactions of alpha-catenin with alpha-actinin and beta-catenin/plakoglobin. *J Cell Sci* 110 (Pt 8): 1013-22
Nitta T, Hata M, Gotoh S, Seo Y, Sasaki H, et al. 2003. Size-selective loosening of the blood-brain barrier in claudin-5-deficient mice. *J Cell Biol* 161: 653-60
Nóbrega CdA, L. P. 2012. Machado-Joseph Disease / Spinocerebellar Ataxia Type 3 In *Spinocerebellar ataxia*, ed. DJ Gazulla. InTech
Oberheim NA, Goldman SA, Nedergaard M. 2012. Heterogeneity of astrocytic form and function. *Methods Mol Biol* 814: 23-45
Onofre I, Mendonca N, Lopes S, Nobre R, de Melo JB, et al. 2016. Fibroblasts of Machado Joseph Disease patients reveal autophagy impairment. *Scientific reports* 6: 28220
Palmer JC, Barker R, Kehoe PG, Love S. 2012. Endothelin-1 is elevated in Alzheimer's disease and upregulated by amyloid-beta. *J Alzheimers Dis* 29: 853-61
Paulson HL. 2007. Dominantly inherited ataxias: lessons learned from Machado-Joseph disease/spinocerebellar ataxia type 3. *Semin Neurol* 27: 133-42

Paulson HL, Das SS, Crino PB, Perez MK, Patel SC, et al. 1997. Machado-Joseph disease gene product is a cytoplasmic protein widely expressed in brain. *Ann Neurol* 41: 453-62
Petty MA, Lo EH. 2002. Junctional complexes of the blood-brain barrier: permeability changes in neuroinflammation. *Prog Neurobiol* 68: 311-23
Poschl E, Schlotzer-Schrehardt U, Brachvogel B, Saito K, Ninomiya Y, Mayer U. 2004. Collagen IV is essential for basement membrane stability but dispensable for initiation of its assembly during early development. *Development* 131: 1619-28
Pozzi C, Valtorta M, Tedeschi G, Galbusera E, Pastori V, et al. 2008. Study of subcellular localization and proteolysis of ataxin-3. *Neurobiol Dis* 30: 190-200
Proctor JM, Zang K, Wang D, Wang R, Reichardt LF. 2005. Vascular development of the brain requires beta8 integrin expression in the neuroepithelium. *J Neurosci* 25: 9940-8
Reina CP, Zhong X, Pittman RN. 2010. Proteotoxic stress increases nuclear localization of ataxin-3. *Hum Mol Genet* 19: 235-49
Reitsma S, Slaaf DW, Vink H, van Zandvoort MA, oude Egbrink MG. 2007. The endothelial glycocalyx: composition, functions, and visualization. *Pflugers Archiv : European journal of physiology* 454: 345-59
Rempe RG, Hartz AM, Bauer B. 2016. Matrix metalloproteinases in the brain and blood-brain barrier: Versatile breakers and makers. *J Cereb Blood Flow Metab* 36: 1481-507
Rite I, Machado A, Cano J, Venero JL. 2007. Blood-brain barrier disruption induces in vivo degeneration of nigral dopaminergic neurons. *J Neurochem* 101: 1567-82
Rochfort KD, Cummins PM. 2015. Cytokine-mediated dysregulation of zonula occludens-1 properties in human brain microvascular endothelium. *Microvasc Res* 100: 48-53
Rodrigues AJ, Coppola G, Santos C, Costa Mdo C, Ailion M, et al. 2007. Functional genomics and biochemical characterization of the C. elegans orthologue of the Machado-Joseph disease protein ataxin-3. *FASEB J* 21: 1126-36
Rodrigues SF, Granger DN. 2015. Blood cells and endothelial barrier function. *Tissue barriers* 3: e978720
Rössner W, Tempel K. 1966. Quantitative determination of the permeability of the so-called blood-brain barrier of Evans blue (T 1824). *Medicina et pharmacologia experimentalis. International journal of experimental medicine* 14: 169
Roura S, Miravet S, Piedra J, Garcia de Herreros A, Dunach M. 1999. Regulation of E-cadherin/Catenin association by tyrosine phosphorylation. *J Biol Chem* 274: 36734-40
Rub U, Brunt ER, Deller T. 2008. New insights into the pathoanatomy of spinocerebellar ataxia type 3 (Machado-Joseph disease). *Curr Opin Neurol* 21: 111-6
Sa-Pereira I, Brites D, Brito MA. 2012. Neurovascular unit: a focus on pericytes. *Mol Neurobiol* 45: 327-47
Sakakibara A, Furuse M, Saitou M, Ando-Akatsuka Y, Tsukita S. 1997. Possible involvement of phosphorylation of occludin in tight junction formation. *J Cell Biol* 137: 1393-401
Sakka L, Coll G, Chazal J. 2011. Anatomy and physiology of cerebrospinal fluid. *Eur Ann Otorhinolaryngol Head Neck Dis* 128: 309-16
Satoh H, Zhong Y, Isomura H, Saitoh M, Enomoto K, et al. 1996. Localization of 7H6 tight junction-associated antigen along the cell border of vascular endothelial cells correlates with paracellular barrier function against ions, large molecules, and cancer cells. *Exp Cell Res* 222: 269-74
Saunders NR, Ek CJ, Habgood MD, Dziegielewska KM. 2008. Barriers in the brain: a renaissance? *Trends Neurosci* 31: 279-86
Scherzinger E, Lurz R, Turmaine M, Mangiarini L, Hollenbach B, et al. 1997. Huntingtin-encoded polyglutamine expansions form amyloid-like protein aggregates in vitro and in vivo. *Cell* 90: 549-58
Schmidt T, Landwehrmeyer GB, Schmitt I, Trottier Y, Auburger G, et al. 1998. An isoform of ataxin-3 accumulates in the nucleus of neuronal cells in affected brain regions of SCA3 patients. *Brain Pathol* 8: 669-79
Schmitt I, Linden M, Khazneh H, Evert BO, Breuer P, et al. 2007. Inactivation of the mouse Atxn3 (ataxin-3) gene increases protein ubiquitination. *Biochemical and biophysical research communications* 362: 734-9
Schubert-Unkmeir A, Konrad C, Slanina H, Czapek F, Hebling S, Frosch M. 2010. Neisseria meningitidis induces brain microvascular endothelial cell detachment from the matrix and cleavage of occludin: a role for MMP-8. *PLoS pathogens* 6: e1000874

Seguin R, Biernacki K, Rotondo RL, Prat A, Antel JP. 2003. Regulation and functional effects of monocyte migration across human brain-derived endothelial cells. *J Neuropathol Exp Neurol* 62: 412-9

Seidel K, den Dunnen WF, Schultz C, Paulson H, Frank S, et al. 2010. Axonal inclusions in spinocerebellar ataxia type 3. *Acta Neuropathol* 120: 449-60

Sequeiros J, Coutinho P. 1993. Epidemiology and clinical aspects of Machado-Joseph disease. *Adv Neurol* 61: 139-53

Shao J, Diamond MI. 2007. Polyglutamine diseases: emerging concepts in pathogenesis and therapy. *Hum Mol Genet* 16 Spec No. 2: R115-23

Shibuya M. 2008. Vascular endothelial growth factor-dependent and -independent regulation of angiogenesis. *BMB reports* 41: 278-86

Simoes AT, Goncalves N, Koeppen A, Deglon N, Kugler S, et al. 2012. Calpastatin-mediated inhibition of calpains in the mouse brain prevents mutant ataxin 3 proteolysis, nuclear localization and aggregation, relieving Machado-Joseph disease. *Brain* 135: 2428-39

Sims DE. 1991. Recent advances in pericyte biology--implications for health and disease. *Can J Cardiol* 7: 431-43

Sixt M, Engelhardt B, Pausch F, Hallmann R, Wendler O, Sorokin LM. 2001. Endothelial cell laminin isoforms, laminins 8 and 10, play decisive roles in T cell recruitment across the blood-brain barrier in experimental autoimmune encephalomyelitis. *J Cell Biol* 153: 933-46

Sole M, Minano-Molina AJ, Unzeta M. 2015. Cross-talk between Abeta and endothelial SSAO/VAP-1 accelerates vascular damage and Abeta aggregation related to CAA-AD. *Neurobiol Aging* 36: 762-75

Song YJ, Halliday GM, Holton JL, Lashley T, O'Sullivan SS, et al. 2009. Degeneration in different parkinsonian syndromes relates to astrocyte type and astrocyte protein expression. *J Neuropathol Exp Neurol* 68: 1073-83

Soong BW, Liu RS. 1998. Regional decrease in brain glucose metabolism in asymptomatic gene carriers of Machado-Joseph disease: a preliminary report. *Zhonghua Yi Xue Za Zhi (Taipei)* 61: 121-6

Speder P, Brand AH. 2014. Gap junction proteins in the blood-brain barrier control nutrient-dependent reactivation of Drosophila neural stem cells. *Developmental cell* 30: 309-21

Stamatovic SM, Johnson AM, Keep RF, Andjelkovic AV. 2016. Junctional proteins of the blood-brain barrier: New insights into function and dysfunction. *Tissue barriers* 4: e1154641

Stamatovic SM, Keep RF, Wang MM, Jankovic I, Andjelkovic AV. 2009. Caveolae-mediated internalization of occludin and claudin-5 during CCL2-induced tight junction remodeling in brain endothelial cells. *J Biol Chem* 284: 19053-66

Steiner E, Enzmann GU, Lyck R, Lin S, Ruegg MA, et al. 2014. The heparan sulfate proteoglycan agrin contributes to barrier properties of mouse brain endothelial cells by stabilizing adherens junctions. *Cell and tissue research* 358: 465-79

Stern L, Gautier R. 1921. Recherches Sur Le Liquide CÉphalo-Rachidien: I.–Les Rapports Entre Le Liquide CÉphalo-Rachidien et la Circulation Sanguine. *Archives Internationales de Physiologie* 17: 138-92

Stevenson BR, Begg DA. 1994. Concentration-dependent effects of cytochalasin D on tight junctions and actin filaments in MDCK epithelial cells. *J Cell Sci* 107 (Pt 3): 367-75

Storck SE, Meister S, Nahrath J, Meissner JN, Schubert N, et al. 2016. Endothelial LRP1 transports amyloid-beta(1-42) across the blood-brain barrier. *J Clin Invest* 126: 123-36

Stratman AN, Malotte KM, Mahan RD, Davis MJ, Davis GE. 2009. Pericyte recruitment during vasculogenic tube assembly stimulates endothelial basement membrane matrix formation. *Blood* 114: 5091-101

Stuart RO, Sun A, Bush KT, Nigam SK. 1996. Dependence of epithelial intercellular junction biogenesis on thapsigargin-sensitive intracellular calcium stores. *J Biol Chem* 271: 13636-41

Stuart RO, Sun A, Panichas M, Hebert SC, Brenner BM, Nigam SK. 1994. Critical role for intracellular calcium in tight junction biogenesis. *J Cell Physiol* 159: 423-33

Sui YT, Bullock KM, Erickson MA, Zhang J, Banks WA. 2014. Alpha synuclein is transported into and out of the brain by the blood-brain barrier. *Peptides* 62: 197-202

Suite ND, Sequeiros J, McKhann GM. 1986. Machado-Joseph disease in a Sicilian-American family. *J Neurogenet* 3: 177-82

Taddei A, Giampietro C, Conti A, Orsenigo F, Breviario F, et al. 2008. Endothelial adherens junctions control tight junctions by VE-cadherin-mediated upregulation of claudin-5. *Nature cell biology* 10: 923-34
Takeichi M. 1995. Morphogenetic roles of classic cadherins. *Curr Opin Cell Biol* 7: 619-27
Takiyama Y, Nishizawa M, Tanaka H, Kawashima S, Sakamoto H, et al. 1993. The gene for Machado-Joseph disease maps to human chromosome 14q. *Nat Genet* 4: 300-4
Thiollier T, Wu C, Contamin H, Li Q, Zhang J, Bezard E. 2016. Permeability of blood-brain barrier in macaque model of 1-methyl-4-phenyl-1,2,3,6-tetrahydropyridine-induced Parkinson disease. *Synapse* 70: 231-9
Tietz S, Engelhardt B. 2015. Brain barriers: Crosstalk between complex tight junctions and adherens junctions. *J Cell Biol* 209: 493-506
Tilling T, Korte D, Hoheisel D, Galla HJ. 1998. Basement membrane proteins influence brain capillary endothelial barrier function in vitro. *J Neurochem* 71: 1151-7
Todi SV, Winborn BJ, Scaglione KM, Blount JR, Travis SM, Paulson HL. 2009. Ubiquitination directly enhances activity of the deubiquitinating enzyme ataxin-3. *EMBO J* 28: 372-82
Torashima T, Koyama C, Iizuka A, Mitsumura K, Takayama K, et al. 2008. Lentivector-mediated rescue from cerebellar ataxia in a mouse model of spinocerebellar ataxia. *EMBO Rep* 9: 393-9
Tornavaca O, Chia M, Dufton N, Almagro LO, Conway DE, et al. 2015. ZO-1 controls endothelial adherens junctions, cell-cell tension, angiogenesis, and barrier formation. *J Cell Biol* 208: 821-38
Trottier Y, Cancel G, An-Gourfinkel I, Lutz Y, Weber C, et al. 1998. Heterogeneous intracellular localization and expression of ataxin-3. *Neurobiol Dis* 5: 335-47
van de Haar HJ, Burgmans S, Jansen JF, van Osch MJ, van Buchem MA, et al. 2016. Blood-Brain Barrier Leakage in Patients with Early Alzheimer Disease. *Radiology* 281: 527-35
van den Berg BM, Nieuwdorp M, Stroes ES, Vink H. 2006. Glycocalyx and endothelial (dys) function: from mice to men. *Pharmacol Rep* 58 Suppl: 75-80
Vorbrodt AW, Dobrogowska DH. 2004. Molecular anatomy of interendothelial junctions in human blood-brain barrier microvessels. *Folia Histochem Cytobiol* 42: 67-75
Waldvogel HJ, Dragunow M, Faull RL. 2015. Disrupted vasculature and blood-brain barrier in Huntington disease. *Ann Neurol* 78: 158-9
Wegmann F, Ebnet K, Du Pasquier L, Vestweber D, Butz S. 2004. Endothelial adhesion molecule ESAM binds directly to the multidomain adaptor MAGI-1 and recruits it to cell contacts. *Exp Cell Res* 300: 121-33
Weiss A, Trager U, Wild EJ, Grueninger S, Farmer R, et al. 2012. Mutant huntingtin fragmentation in immune cells tracks Huntington's disease progression. *J Clin Invest* 122: 3731-6
Weiss N, Miller F, Cazaubon S, Couraud PO. 2009. The blood-brain barrier in brain homeostasis and neurological diseases. *Biochimica et biophysica acta* 1788: 842-57
Wilhelm I, Fazakas C, Krizbai IA. 2011. In vitro models of the blood-brain barrier. *Acta Neurobiol Exp (Wars)* 71: 113-28
Willott E, Balda MS, Heintzelman M, Jameson B, Anderson JM. 1992. Localization and differential expression of two isoforms of the tight junction protein ZO-1. *Am J Physiol* 262: C1119-24
Winkler EA, Bell RD, Zlokovic BV. 2011. Central nervous system pericytes in health and disease. *Nature neuroscience* 14: 1398-405
Winkler EA, Sagare AP, Zlokovic BV. 2014. The pericyte: a forgotten cell type with important implications for Alzheimer's disease? *Brain Pathol* 24: 371-86
Wolburg H, Lippoldt A. 2002. Tight junctions of the blood-brain barrier: development, composition and regulation. *Vascul Pharmacol* 38: 323-37
Xiao G, Gan LS. 2013. Receptor-mediated endocytosis and brain delivery of therapeutic biologics. *International journal of cell biology* 2013: 703545
Yan J, Fu Q, Cheng L, Zhai M, Wu W, et al. 2014. Inflammatory response in Parkinson's disease (Review). *Mol Med Rep* 10: 2223-33
Yates RL, Esiri MM, Palace J, Jacobs B, Perera R, DeLuca GC. 2017. Fibrin(ogen) and neurodegeneration in the progressive multiple sclerosis cortex. *Ann Neurol* 82: 259-70
Yong VW. 2005. Metalloproteinases: mediators of pathology and regeneration in the CNS. *Nat Rev Neurosci* 6: 931-44
Yu YC, Kuo CL, Cheng WL, Liu CS, Hsieh M. 2009. Decreased antioxidant enzyme activity and increased mitochondrial DNA damage in cellular models of Machado-Joseph disease. *Journal of neuroscience research* 87: 1884-91

Yurchenco PD. 2011. Basement membranes: cell scaffoldings and signaling platforms. *Cold Spring Harbor perspectives in biology* 3

Zlokovic BV. 2008. The blood-brain barrier in health and chronic neurodegenerative disorders. *Neuron* 57: 178-201

Zlokovic BV. 2011. Neurovascular pathways to neurodegeneration in Alzheimer's disease and other disorders. *Nat Rev Neurosci* 12: 723-38